Volume 12
Number 24
28 June 2021
Pages 8271–8572

Chemical Science

rsc.li/chemical-science

ISSN 2041-6539

ROYAL SOCIETY OF CHEMISTRY

REVIEW ARTICLE

Bo Peng, Lin Li, Shao Q. Yao *et al.*

Recent advances in activity-based probes (ABPs) and affinity-based probes (A*f*BPs) for profiling of enzymes

Chemical Science

ROYAL SOCIETY OF CHEMISTRY

REVIEW

View Article Online
View Journal | View Issue

Cite this: *Chem. Sci.*, 2021, **12**, 8288

Recent advances in activity-based probes (ABPs) and affinity-based probes (*A*fBPs) for profiling of enzymes

Haixiao Fang,[a] Bo Peng,*[b] Sing Yee Ong,[c] Qiong Wu,[a] Lin Li *[a] and Shao Q. Yao *[c]

Activity-based protein profiling (ABPP) is a technique that uses highly selective active-site targeted chemical probes to label and monitor the state of proteins. ABPP integrates the strengths of both chemical and biological disciplines. By utilizing chemically synthesized or modified bioactive molecules, ABPP is able to reveal complex physiological and pathological enzyme–substrate interactions at molecular and cellular levels. It is also able to provide critical information of the catalytic activity changes of enzymes, annotate new functions of enzymes, discover new substrates of enzymes, and allow real-time monitoring of the cellular location of enzymes. Based on the mechanism of probe-enzyme interaction, two types of probes that have been used in ABPP are activity-based probes (ABPs) and affinity-based probes (*A*fBPs). This review highlights the recent advances in the use of ABPs and *A*fBPs, and summarizes their design strategies (based on inhibitors and substrates) and detection approaches.

Received 8th March 2021
Accepted 11th May 2021

DOI: 10.1039/d1sc01359a

rsc.li/chemical-science

Introduction

Enzymes are a specialized class of proteins characterized by their remarkable catalytic specificity and efficiency. They represent an extremely important class of biological catalysts that are indispensable for signal transduction and regulation of cellular activities.[1] Therefore, understanding the roles of various enzymes involved in mammalian physiological and pathological processes is essential in providing critical information for drug discovery and disease diagnosis.[2,3] In order to directly monitor enzymatic activities *in cellulo* and *in vivo*, there is an urgent need in the field of proteomics to isolate them from complex biosystems for labeling and enrichment identification purposes.[4] Activity-based protein profiling (ABPP) is a chemical proteomic technique that uses small-molecule probes to directly understand the functional state of enzymes in biological systems,[5,6] and is gradually becoming one of the major techniques in proteomics due to its ability to fill the gaps of other proteomic approaches.

Developed by Benjamin F. Cravatt and Matthew Bogyo in the late 1990s,[7,8] ABPP employs activity-based probes (ABPs) to specifically label proteins in biological samples.[9] These ABPs are designed to covalently modify the active site of the target enzyme (or a family of enzymes) in a highly selective manner.[10] Successful ABPP relies on the critical design and synthesis of the chemical probes. Most ABPs share a similar basic design, which usually includes a reactive group (or warhead, WH), a reporter group, and a linker (Fig. 1A). Reactive groups are often derived from known covalent inhibitors of the target enzyme. Commonly used reporter groups are fluorescent dyes and biotin (Fig. 1B) that allow labeled proteins to be visualized and enriched for subsequent studies. The linker can be a hydrophilic chain, a lipophilic chain or a peptide, in which its basic function is to provide adequate space between the reactive and the reporter groups.

Improper installation of the bulky biotin and fluorescent reporter groups, however, significantly affects the activity and cell permeability of the probes, thereby limiting their applications in living cells. The use of highly selective and reliable bioorthogonal chemistry involving small functional groups is able to overcome the above-mentioned shortcomings.[11,12] Commonly used bioorthogonal reactions include copper(I)-catalyzed azide–alkyne cycloaddition (CuAAC),[13] copper-free strain-promoted azide–alkyne cycloaddition (SPAAC)[14] and inverse electron-demand Diels–Alder (iEDDA)[15] (Fig. 1C). This new generation of ABPs carries a suitable bioorthogonal handle, and upon covalent attachment to their targets, a reporter group is then introduced to the labeled targets *via* bioorthogonal reaction.

In most studies, ABPs are derived from covalent inhibitors of a target protein. For proteins that lack covalent inhibitors, photoaffinity labeling (PAL) offers a way to study their interactions. Since its development by Westheimer *et al.* in 1962,[16] the use of PAL, or photo-crosslinking, has seen a dramatic increase

[a]*Key Laboratory of Flexible Electronics (KLOFE), Institute of Advanced Materials (IAM), Nanjing Tech University (NanjingTech), 30 South Puzhu Road, Nanjing, 211816, P. R. China. E-mail: iamlli@njtech.edu.cn*

[b]*Frontiers Science Center for Flexible Electronics, Xi'an Institute of Flexible Electronics (IFE), Xi'an Institute of Biomedical Materials & Engineering, Northwestern Polytechnical University, 127 West Youyi Road, Xi'an 710072, P. R. China. E-mail: iambpeng@nwpu.edu.cn*

[c]*Department of Chemistry, National University of Singapore, 4 Science Drive 2, 117544, Singapore. E-mail: chmyaosq@nus.edu.sg*

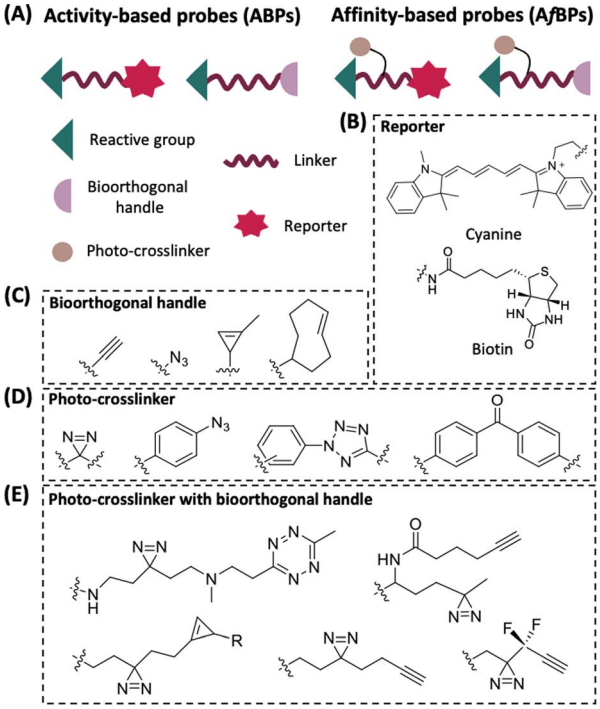

Fig. 1 General components of ABPs and AfBPs (A) and structures of commonly used reporter groups, bioorthogonal handles and photo-crosslinkers. (B) Examples of the reporter groups: cyanine fluorophore for visualization and biotin as an affinity tag. (C) Examples of commonly used bioorthogonal handles in ABPP. (D) Examples of photo-crosslinkers that are commonly used in ABPP. (E) Examples of photo-crosslinkers with bioorthogonal handles for AfBPs.

in proteomic research. Upon ultraviolet (UV) irradiation, the photo-crosslinking group generates a highly reactive intermediate that reacts with its adjacent molecule, resulting in the formation of a covalent bond between the probe and the target protein (Fig. 1A). This class of PAL-based probes is also being referred to as affinity-based probes (AfBPs).[17] Amongst the various types of photo-crosslinkers, arylazides,[18] benzophenones,[19] and diazirines[20] are most commonly employed in AfBPs (Fig. 1D and E). Recently, a new type of photo-crosslinker, diaryltetrazole (Fig. 1D),[21] was developed by our group that has shown a unique photo-crosslinking mechanism and could effectively reduce background labeling with excellent cross-linking efficiency.[22,23]

Depending on the types of functional groups on the probes, the workflow of protein profiling could proceed in different ways (Fig. 2). ABPP using ABPs is a covalent-based protein profiling method that is mainly limited by the choice of reactive groups, and therefore is difficult to profile a wide range of proteins. On the other hand, ABPP using AfBPs suffers from non-specific interferences caused by background protein labeling, and therefore is difficult to reliably identify target proteins. In order to overcome these existing limitations, we and others have developed highly effective "minimalist" photo-crosslinkers that could be conveniently introduced into probes and for subsequent use in quantitative mass spectrometry-based proteomics research and highly accurate large-scale target identification (Fig. 1E).[24–28]

With the rapid development of ABPP in the field of proteomics, an increasing number of advanced ABPP strategies have emerged to expand its applications. Advanced strategies such as isotopic tandem orthogonal proteolysis-ABPP (isoTOP-ABPP),[29] fluopol-ABPP high-throughput screening (fluopol-ABPP HTS),[30] reverse-polarity ABPP (RP-ABPP)[31] and near-infrared quenched fluorescent ABPP (NIR*q*-ABPP)[32] have since been applied for protein active-site identification, ligand discovery and tissue imaging.

In this review, we summarize the recent advances (from 2016 to present) made in the use of inhibitor- and substrate-based ABPs and AfBPs for proteome-wide enzyme profiling. Their probe designs and applications in drug target discovery and

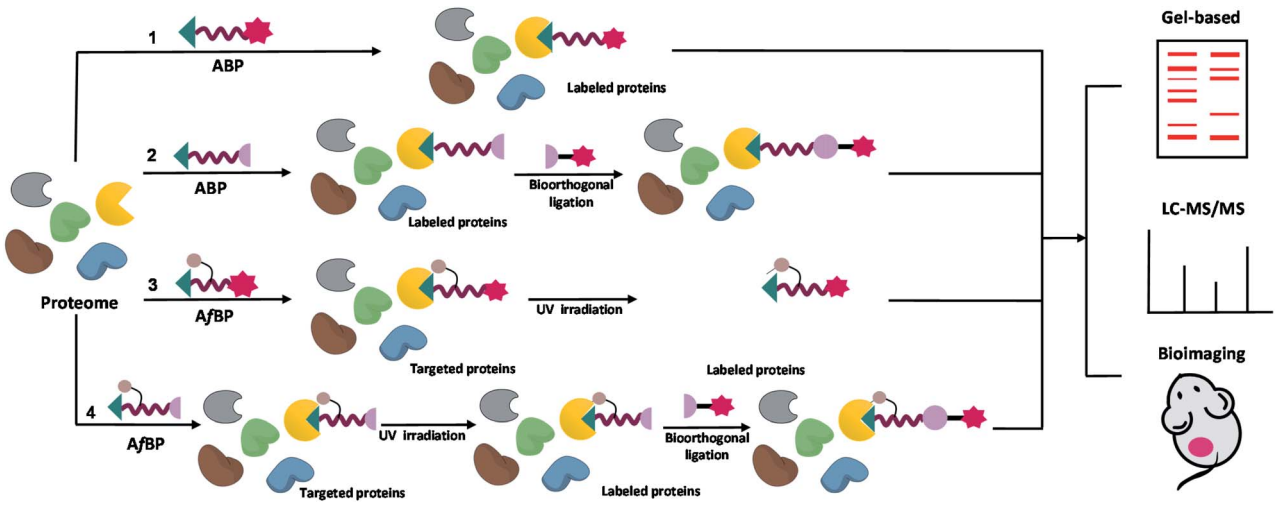

Fig. 2 The general workflow of ABPP using ABPs and AfBPs, from identification to subsequent enrichment and quantification of target proteins. Target identification using ABPs without (1) and with (2) a bioorthogonal reporter. Target identification using AfBPs without (3) and with (4) a bioorthogonal reporter. ABP-modified proteins can be detected and identified using a variety of biochemical and cell biological techniques including gel-based fluorescence analysis, mass spectrometry-based analysis and bioimaging.

biological studies of enzyme function are also discussed. Finally, we end this review by describing our perspectives and proposing future developments of ABPP.

Inhibitor-based ABPs and A*f*BPs for enzymes

Enzymes play a critical role in physiological functions such as enabling intricate processes of cell metabolism to proceed in an orderly fashion and maintaining cell metabolism at normal physiological functions. Enzyme overexpression has been widely observed in many diseases.[33,34] The inhibition of disease-related enzymatic activities, therefore, offers great therapeutic opportunities. For this reason, tremendous efforts have been devoted to the development of enzyme inhibitors.[35,36] The application of ABPP by using probes which are designed on the basis of enzyme inhibitors could allow the rapid identification of potential off-targets, thereby providing important and valuable information for drug discovery and optimization. In addition, these probes could also help to delineate the intracellular distribution of target enzymes and discover their novel biological functions.

Kinase inhibitor-based probes

Kinases are an essential class of enzymes critically involved in most signal transduction pathways. Over the years, many human malignancies have been found to be associated with the dysfunction and/or dysregulation of kinases. Consequently, many kinases have been attractive targets of drug discovery and development for years.[37] The use of known kinase inhibitors as the basis in the design of kinase-based ABPs is a widely used strategy.

Bruton's tyrosine kinase (BTK) plays an important role in tumorigenesis and it is essential for the survival of various B-cell malignancies including leukemia.[38] The BTK inhibitor, ibrutinib, inhibits BTK by forming a covalent bond with a Cys residue in the active site of BTK.[39] Chen *et al.* reported a BTK-selective ABP **1** based on ibrutinib (Fig. 3A).[40] By using **1** in an enzyme-linked immunosorbent assay (ELISA) method, the authors were able to use the probe for quantification of endogenous levels of BTK from living cells. Similarly, Wang *et al.* reported a series of ABPs having different bioorthogonal handles, which were constructed by conjugating maleimide-coumarin to ibrutinib.[41] Upon *in vitro* and *in situ* screenings, the authors found that one of the four ABPs (**2**, Fig. 3A) displayed high sensitivity and selectivity towards BTK (Fig. 3B).

Epidermal growth factor receptor (EGFR) is a member of the receptor tyrosine kinase (RTK) family. Mutations and overexpression of EGFR are closely associated with tumor pathogenesis.[42] In 2017, Planken *et al.* developed a new EGFR inhibitor (PF-06747775)[43] based on PF-06459988, an irreversible EGFR T790M mutant inhibitor. ABPs **3** and **4** (Fig. 3A) were designed on the basis of two EGFR inhibitors, PF-06747775 and PF-06459988. The proteome-wide reactivity of **3** was demonstrated to be lower than that of **4** by spectroscopic experiments,

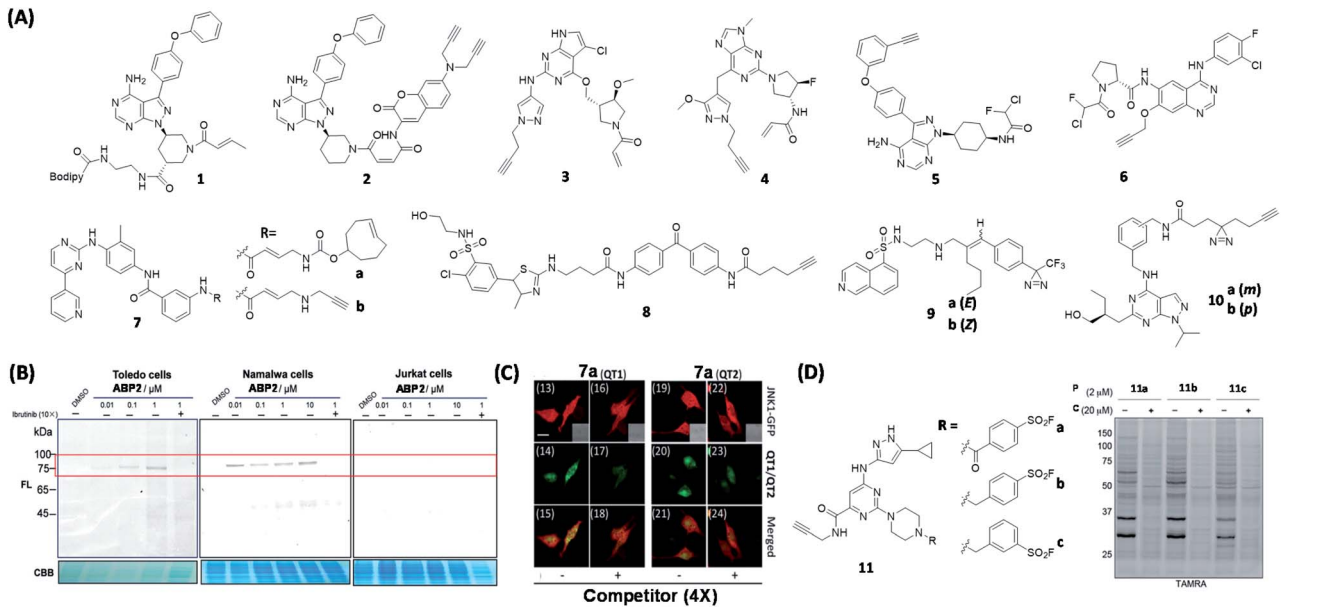

Fig. 3 Kinase inhibitor-based ABPs and A*f*BPs and their *in cellulo* applications. (A) Reported kinase inhibitor-based ABPs and A*f*BPs. (B) Gel-based labeling of BTK with **2** in BTK-positive (Toledo, Namalwa) and BTK-negative cells (Jurkat), only positive cells showed a band around 75 kDa which demonstrated the successful labeling of cellular BTK. Reproduced from ref. 41 with permission from Royal Society of Chemistry, copyright 2019. (C) Imaging of JNK1-GFP-transfected HeLa cells using **7a** with two TP reporters, both of which successfully labeled JNK1 in living cells. Reproduced from ref. 48 with permission from Royal Society of Chemistry, copyright 2019. (D) Reported sulfonyl fluoride-based ABPs for kinases (left). In-gel fluorescence analysis of Jurkat cells treated with either DMSO or the probe competitor, followed by treatment with **11a** to **11c**. **11** was successfully used for broad-spectrum kinase labeling in cells. P = probe, C = competitor. Reproduced from ref. 53 with permission from American Chemical Society, copyright 2017.

highlighting the superior specificity of **3**. The results also indicated that, in addition to the T790M mutant of EGFR, **3** displayed a higher inhibitory effect on both exon19-deletion (Del) and L858R mutants when compared to the wild-type EGFR.

A number of proteomic studies have shown that several types of acrylamide-based kinase inhibitors exhibited off-target protein labeling in the submicromolar to micromolar concentration ranges.[44] For example, ibrutinib was found to inhibit other members of the Tec kinase family that contain a critical Cys residue in the kinase domain.[45] This off-target activity often results in unwanted toxicity. Ojida's group synthesized a series of ABPs by attaching α-chlorofluoroacetamide (CFA) as a WH, together with a handle, to two kinase inhibitors, ibrutinib and afatinib (EFGR inhibitor), giving probes **5** and **6** (Fig. 3A), respectively.[46] Subsequent proteome-wide protein profiling experiments indicated that **5** and **6** were able to inhibit BTK and EGFR, respectively, with low off-target activity. These results thus demonstrate the potential of using the highly specific CFA as a new covalent inhibitor WH.

c-Jun N-terminal kinase (JNK) is critically involved in many important stress signaling pathways, and its dysregulation is closely associated with many pathological states.[47] Inspired by the discovery of the first irreversible JNK inhibitor (JNK-IN-8) having nanomolar inhibitory activity and high selectivity, our group developed JNK ABPs **7a** & **7b** (Fig. 3A) based on the structure of JNK-IN-8.[48] We subsequently carried out proteome-wide reactivity profiling, as well as live-cell bioimaging (Fig. 3C), with these probes together with different two-photon (TP) fluorescence reporters, to detect endogenous JNKs from live mammalian cells.

By using a benzophenone photo-crosslinker, Desrochers *et al.* synthesized A*f*BP **8** (Fig. 3A) for phosphatidylinositol 4-kinases B (PI4KB) based on the PIK inhibitor, PIK93.[49] PI4KB, which belongs to the PIK family, can be recruited to the Golgi membrane for activation and subsequent phosphorylation through protein–protein interactions.[50] The authors used **8** to study the role of PI4KB in hepatitis C virus (HCV) infection by simultaneously tagging PI4KB-interacting Golgi recruitment protein, ACBD3. This work demonstrates the use of A*f*BP as a tool to study the role of ribonucleic (RNA) viruses *via* the disruption of PIK regulation.

In another study, Overkleeft's group reported A*f*BPs **9a** & **9b** (Fig. 3A) based on the protein kinase A (PKA) inhibitor, H89.[51] Gel-based experiments revealed that **9a** having a (*E*)-configuration (same as that in H89) could effectively label both PKA and protein kinase B-α (AKT1). In contrast, **9b** having a (*Z*)-configuration had a diminished AKT1 inhibition/labeling effect. This study shows that there is a peripheral difference between the two kinases, hence providing useful information for the future design of AKT1-selective molecules.

Recently, Bush *et al.* developed a set of pan-/cyclin-dependent kinases (CDK) A*f*BPs based on the pan-CDK inhibitor, roscovitine.[52] The optimal probes **10a** & **10b** (Fig. 3A) containing an alkyl diazirine were modified to include an alkyne bioorthogonal handle, and **10b** was found to enrich 5 CDKs as well as 12 other kinases.

Sulfonyl fluoride is an electrophilic functional group that is resistant to hydrolysis and can react with nucleophilic sites found in a variety of proteins. Taunton's group designed a series of probes (**11**, Fig. 3D) based on a pyrimidine 3-aminopyrazole scaffold bearing different phenylsulfonyl fluoride substituents.[53] By performing proteome-wide screening, the authors found that **11** could covalently label a broad range of intracellular kinomes with high efficiency. The optimized ABP **11b** was able to efficiently compete with high intracellular concentrations of adenosine triphosphate (ATP) in kinase binding, and covalently modify up to 133 endogenous kinases (Fig. 3D). More recently, other sulfonyl fluoride-based probes have also been reported, capable of Lys-selective covalent labeling of proteins such as eIF4E (eukaryotic initiation factor 4E) and Hsp90 (a heat shock protein).[54,55]

Protease inhibitor-based probes

Abnormal protease activities have been implicated in the pathogenesis of many human diseases such as cancer, osteoporosis and arthritis.[56] As a result, proteases represent another class of biological targets that have received much attention in recent years. The very nature of the enzymatic reaction (*i.e.* substrate cleavage) endowed by proteases provides unique opportunities to the development of probes for various purposes, including proteome-wide profiling and imaging of protease activities. Based on this, the concept of quenched fluorescent activity-based probes (*q*ABPs) was first introduced by Bogyo in 2005 (Fig. 4A).[57] *q*ABPs belong to a sub-class of ABPs, and are usually composed of three parts: a fluorophore, a fluorescence quencher and a protease inhibitor. We designed another series of modular *q*ABPs, which contains a mandelic acid core surrounded by a fluorophore, a quencher and an enzyme substrate WH (Fig. 4B).[58] When the probe is introduced into the cell, its WH is enzymatically cleaved leading to the release of the quenched moiety that can sensitively report endogenous enzyme activity through three possible pathways of achieving fluorescent signal amplification. Among them, pathway 3 is the most efficient way (Fig. 4B). As pathway 3 causes the release of a large amount of quencher and highly fluorescent intermediate to diffuse out of the active site of the enzyme, while allowing the labeling of nearby available nucleophiles, such as proteins that are in the same subcellular organelle as the target. The unique feature of such probes is that they emit fluorescent Turn-ON signals only upon the covalent attachment to the target enzyme *via* specific enzymatic reaction. Therefore, this design allows no-wash bioimaging of the activity and cellular localization of target enzyme both *in vitro* and *in vivo*, and with high resolution.

Recently, Bogyo's group extended the concept of *q*ABP by using protease substrates as parts of the probe design (Fig. 5A);[59] the authors developed multivariate "AND-gate" probes containing specific protease substrate sequences which were shown to improve the overall tumor selectivity. These probes (**12** & **13**, Fig. 5B) will only be activated to produce a fluorescent signal upon the cleavage of both substrate sequences by their respective proteases and were subsequently

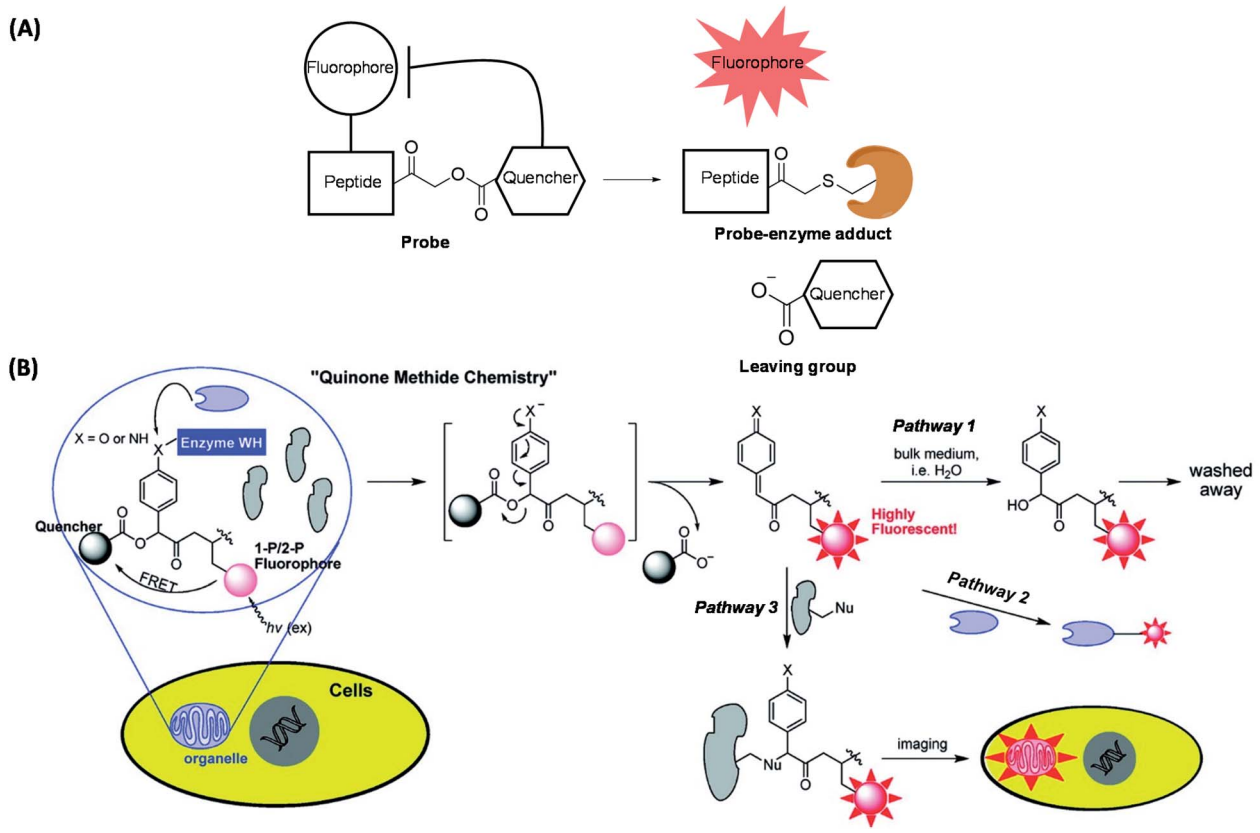

Fig. 4 Two *q*ABP working strategies. (A) Schematic illustration of activity-dependent fluorescent labeling of Cys proteases by using *q*ABP. (B) Another strategy of the enzyme activity-dependent *q*ABP reaction. The structure of *q*ABP contains a mandelic acid core which was surrounded by a fluorophore (red), a quencher and an enzyme WH (blue). The resulting intermediate of enzymatic reaction has three possible pathways within the cells: (pathway 1) hydration/quenching by water; (pathway 2) covalent attachment to the target enzyme; (pathway 3) accumulation in the organelle where the enzymatic reaction occurs. Reproduced from ref. 58 with permission from American Chemical Society, copyright 2011.

used to highlight tumor margins in multiple mouse models of cancer.

Several protease-targeting ABPs have recently been used successfully in animal models for various biological and medical applications including in image-guided surgical removal of tumors. Caspases and cathepsins are important proteases found in all animals and other organisms. Caspase-3 (Casp3, a Cys protease) is one of the key caspases that play a major role in cell apoptosis.[60] Cathepsin B, is another key Cys protease known to be closely associated with tumor infiltration.[61] Previously reported Casp3 probes having a DEVD-based sequence interacted with both cathepsin B and legumain (also a Cys protease).[62,63] In an effort to improve target specificity amongst these three Cys proteases, Blum's team performed further probe optimization by using sequential screening to identify highly specific Casp3 ligands.[64] Trp and Phe were reported to have weak legumain interactions,[65] hence peptides were synthesized to include EWD (Glu–Trp–Asp), EPD (Glu–Pro–Asp) and EFD (Glu–Phe–Asp) sequences. Different lengths of diamino linkers and various quenchers were conjugated in the prime site of LE28.[63] *In vitro* inhibitory activity assays indicated that the replacement of P2 Pro with Phe decreases the binding affinity to legumain but retains the activity against Casp3. Subsequently, the EFD sequence was used to develop *q*ABPs. The bulky quencher (BBQ) was attached to the position close to acyloxymethyl ketone group (AOMK, a well-known Cys protease-targeting WH) to cause a spatial conflict with the main site of cathepsin B. Upon proteome-wide profiling, the resulting *q*ABP **14** (Fig. 6A) was found to be virtually free of labeling by both cathepsin B and legumain (Fig. 6B).

Protease substrate screening in the design of selective probes is a powerful tool for many targets of interest. In 2019, Salvesen *et al.* employed two peptide-based chemical libraries for dissecting the preferences of cathepsin B at P1, P2, P3 and P4 positions.[66] One of the AOMK-based inhibitors that exhibited the highest selectivity in the screen was further functionalized with a Cy5 dye to generate a highly selective ABP for cathepsin B (**15**, Fig. 6A). The authors further demonstrated that **15** could selectively label cathepsin B in an array of 18 human cancer cell lines and non-small lung cancer cells from patients (Fig. 6C).

Based on a previously reported synthesis of depalmitoylase-specific fluorogenic peptide library,[67] Bogyo and coworkers recently reported a similar method that could be used to screen for tumor extract-specific sequence by using a hybrid combinatorial substrate library called HyCoSuL.[68] By identifying the different combinations of natural and non-natural amino acid

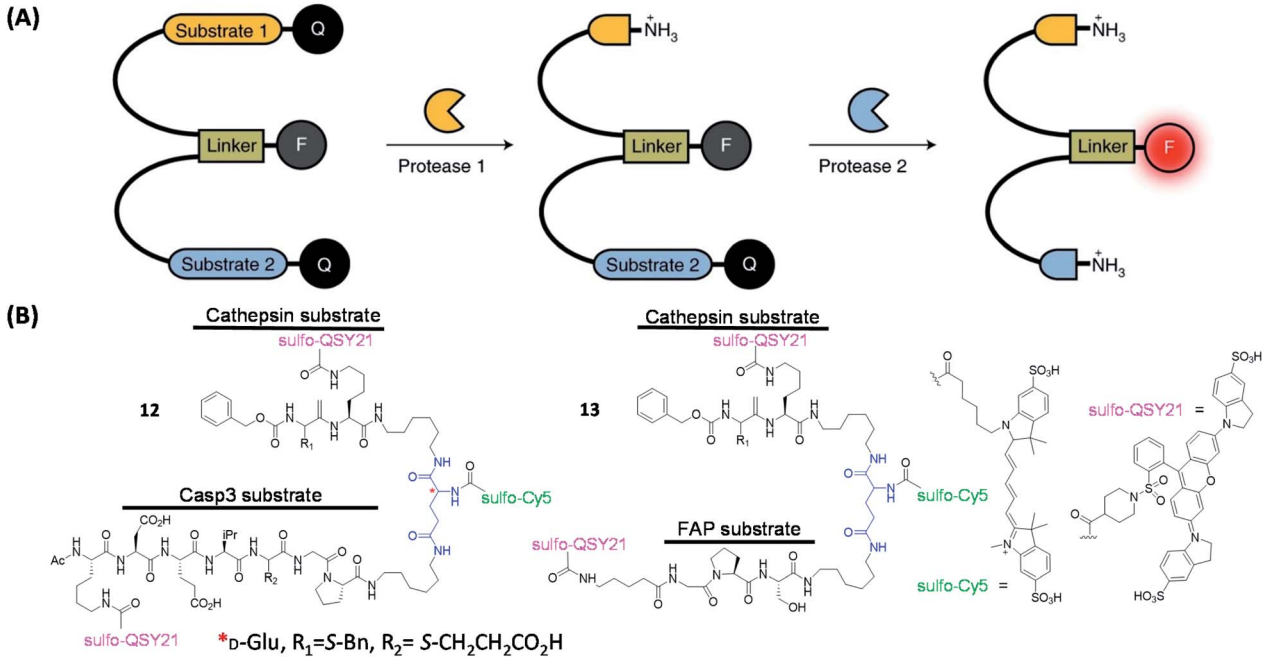

Fig. 5 The working strategies and structures of the "AND-gate" probes. (A) Schematic illustration of an AND-gate fluorescent probe. Q = quencher, F = fluorophore. Reproduced from ref. 59 with permission from Springer Nature, copyright 2020. (B) Structures of reported AND-gate probes.

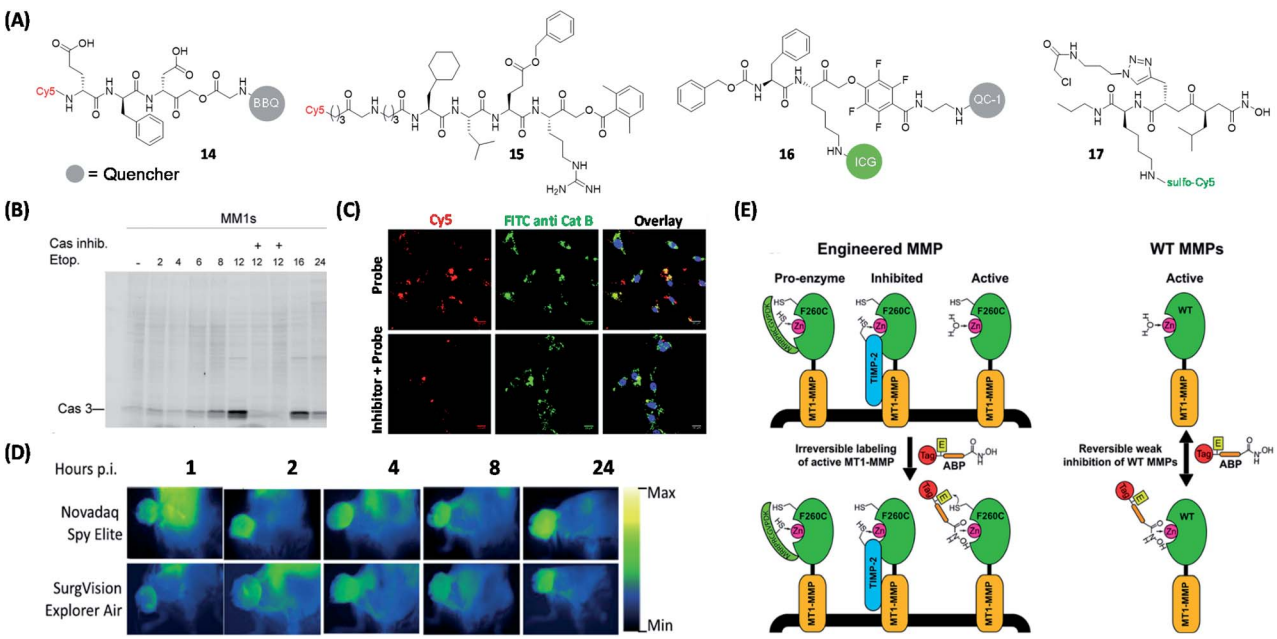

Fig. 6 Protease *q*ABPs for visual labeling of different proteases in live cells and mouse tumors. (A) Structures of reported ABPs to study proteases. (B) In-gel fluorescence analysis of Casp3 in MM1s cells treated with **14**. The addition of Casp3 inhibitor blocked the labeling of Casp3 by the probe, which demonstrated the specificity of the probe to Casp3. Reproduced from ref. 64 with permission from Royal Society of Chemistry, copyright 2016. (C) Labeling of cathepsin B in non-small lung cancer cells from patient using **15** and anti-cathepsin B FITC antibody. The labeling of cathepsin B using **15** was blocked by the addition of cathepsin B inhibitor, but the inhibitor did not influence the labeling efficiency of the antibody. Reproduced from ref. 66 with permission from Royal Society of Chemistry, copyright 2019. (D) Still images from Novadaq Spy Elite and SurgVision Explorer Air of 4T1 tumors at different time points after injection of **16**, which showed the potential of **16**. Reproduced from ref. 69 with permission from Springer, copyright 2020. (E) Specific labeling of active MMP-14 using protein engineering coupled with **17**. The ABP only labeled active MMPs and cannot label enzymes that are inaccessible to zinc or their inhibitory forms. Reproduced from ref. 75 with permission from American Chemical Society, copyright 2018.

residues, "hits" peptide sequences were subsequently taken to construct the corresponding ABPs for tumor-associated enzymes (*e.g.* proteases).

Recently, Popkin's group also developed a tumor-visualization platform by using fluorescent probes in human keratinocyte carcinoma excision specimens.[69] By using a near-infrared protease-targeting *q*ABP that was previously reported by Bogyo *et al.*,[70] the authors successfully applied the platform for rapid and convenient global assessment of margins during skin cancer resection. Suurs *et al.* successfully utilized cathepsin *q*ABP for surgical guidance (**16**, Fig. 6A).[71] This new *q*ABP was synthesized by modifying a previously reported cathepsin *q*ABP;[72] by replacing the original fluorophore and the quencher with an FDA-approved indocyanine green (ICG) dye and QC-1, respectively. The resulting probe was found to be specifically activated by cathepsin X, B/L and S. With the help of a combination of different optical fluorescence imaging camera systems, probe **16** was shown to be able to delineate tumor tissues with high precision during surgery (Fig. 6D).

As a type of zinc-dependent endopeptidases, matrix metalloproteinases (MMPs) play a critical part in cancer pathology.[73] Among them, MMP-14 (MT1-MMP) is considered the main protease involved in the transformation of tumor cells to invasive carcinoma. Based on a previous work,[74] Bogyo's team designed ABP **17** based on a new isobutylsuccinylhydroxamic acid motif (Fig. 6A). ABP **17** was engineered to orthogonally bind to an engineered MMP that contained a Cys residue near the active site of the enzyme (having an active site-bound zinc; Fig. 6E).[75] In addition, the probe has a reversible weak inhibition of WT MMPs. From protein profiling and cell imaging experiments, the authors found that, in the tumor tissue microenvironment, activation of MMP14 was mainly associated with advanced tumors, their surrounding and activated stromal cell populations.

Carbohydrate inhibitor-based probes

Glycosidases (or glycoside hydrolases) are a class of enzymes that hydrolyze glycosidic bonds and play important roles in protein post-translational glycosylation in various organisms.[76] The main hydrolysis product of glucosidases is glucose, which is an indispensable part of glucose metabolism. Depending on the type of glycosidic bonds they hydrolyze, glucosidases can be classified as α- or β-glucosidases. Based on the configuration of the heterotrimeric carbon in the hydrolyzed glucosyl group, glucosidases can also be divided into retaining and inverting glucosidases.[77] Most glucosidases are retaining glucosidases and their catalysis usually involves a two-step mechanism mediated by key catalytic residues including a nucleophilic residue and a pair of general acid/base.[78] Their catalytic reaction proceeds through a covalent glycosyl–enzyme intermediate, in which the carbon configuration of the glycosyl molecule is flipped twice. On the other hand, such conformational secondary flipping does not occur in inverting glucosidases, leading to formation of products with different configurations.[79] To target retaining glycosidases, capturing the covalent intermediates of glycosidic reactions thus became the basis in the design of most inhibitors and ABPs (**18–22**, Fig. 7A), with suitable reporter groups that have been successfully used in various probe designs (Fig. 7B).[80–86] Cyclophellitol-derived epoxides and aziridines are common inhibitors of retaining glucosidases. Upon binding to the retaining glucosidases, their catalytic nucleophile attacks the epoxide/aziridine and generates covalent enzyme-inhibitor adducts.

In 2010, Witte *et al.* reported ABPs **18** that could label glucocerebrosidase (GBA) *in situ* for the first time by linking reporter groups to cylcophellitol.[86] Such a class of ABPs exhibited superior properties over the previously widely used tagged deoxyfluorosugars.[87,88] Therefore selective labeling of a specific type of glycosidase was achieved. The loss of enzymatic activity in GBA is known to cause lysosomal storage impairment, eventually leading to Gaucher disease.[89] Human recombinant GBA (hrGBA) is currently an approved protein-based drug for the treatment of Gaucher disease. Recently, Meel *et al.* successfully labeled hrGBA and endogenous GBA by using **18a** and **18b**, respectively, in normal human dermal fibroblasts (NHDFs) which express the mannose receptor (Man-R) (Fig. 7C).[90] Galactosylceramidase (GALC) is a glycosidase mainly located in the lysosome and is responsible for galactose ceramide hydrolysis. A deficiency in GALC causes Krabbe disease.[91] In 2017, Overkleeft's group reported ABPs **23** (Fig. 7A) for the specific labeling of GALC.[92] These ABPs consist of the β-galactopyranose-configured cyclophellitol-epoxide core that is responsible for conferring specificity to GALC. ABP **23b** was used in the *in situ* imaging of active GALCs in mouse brains. Based on a previous finding that substituting the C8 position of cyclophellitol with bulky groups was effective in generating GBA-selective inhibitors,[93] Wu *et al.* recently reported β-glucuronidase-specific ABPs **24** (Fig. 7A), which allowed rapid and quantitative visualization of *exo*-acting β-glucuronidase (GUSB) and *endo*-acting heparanase (HPSE) from human tissue lysates.[94] One of the best-performing probes, **24c**, was developed by introducing a spacer between the Cy5 dye and aziridine nitrogen, and oxidizing the C6-equivalent position of cyclophellitol to mimic the carboxylate group in glucuronide (GlcUA).

Lysosomal α-glucosidase (GAA) is a retaining α-glucosidase, low levels of GAA expression are known to cause glycogen storage disease type II, also known as Pompe disease.[95] Overkleeft's group found that α-glucose-configured nitrogen-substituted cyclophellitol aziridines could specifically label GH31 retaining α-glucosidases.[96] Therefore, a set of fluorophore- or biotin-modified ABPs (**25**, Fig. 7A) were designed on the basis of α-glucose-configured *N*-alkyl cyclophellitol aziridines for successful monitoring of GH31 retaining α-glucosidase. Amongst the various ABPs, **25a** was shown to be able to quantitatively report the endogenous level of GAA in cell lysates of patients diagnosed with Pompe disease. Recently, the same group also found that ABPs derived from maltose analogues (**26**, Fig. 7A) showed excellent labeling specificity towards retaining α-amylases. These probes thus could potentially be used for the screening of α-amylase inhibitors.[97]

In 2019, Schröder *et al.* detected and differentiated β-xylosidases and *endo*-β-1,4-xylanases in the secretome of *A. niger* by

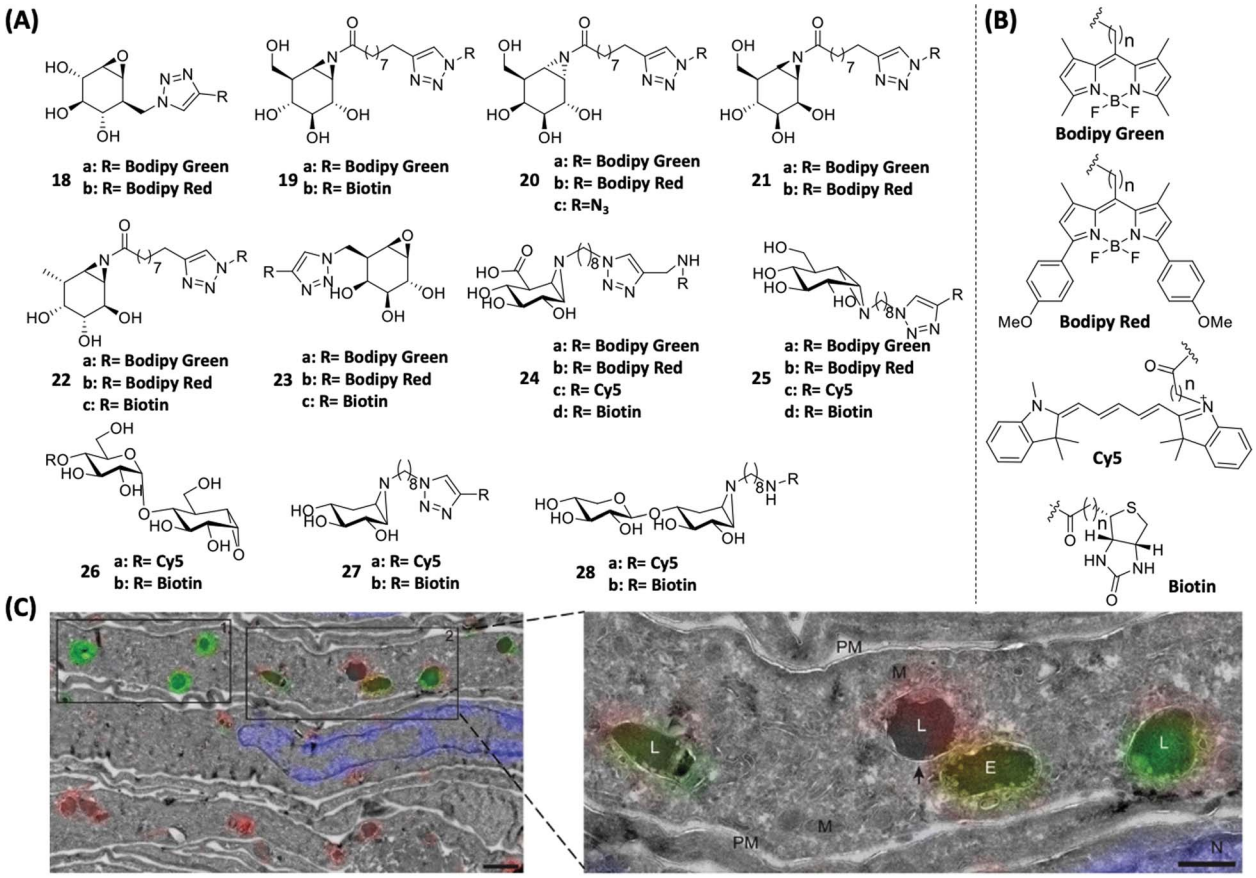

Fig. 7 Inhibitor-based ABPs for glycosidases and labeling of GBA and hrGBA in human tissues by using ABPs. (A) Structures of cyclophellitol-derived epoxides- and aziridines-based ABPs. (B) Structures of various reporter groups used in ABPs. (C) Overlay of electron micrographs and confocal fluorescence images of NHDF ultrathin cryosections expressing Man-R. The metabolic processes of hrGBA and endogenous GBA *in vivo* were traced using **18**. **18a**-labeled hrGBA (green), **18b**-labeled endogenous GBA (red) and nuclei labeled with DAPI (blue). E = endosome; L = lysosome. M = mitochondria; PM = plasma membrane. Reproduced from ref. 90 with permission from Wiley-VCH GmbH, copyright 2019.

using ABPs **27** and **28** (Fig. 7A), respectively.[98] Fluorescence labeling and proteomic analysis revealed that *A. niger* secreted different catabolic enzymes according to the carbon source used in its growth process.

ABPP has also been used as a tool to study gut flora. Whidbey *et al.* developed a platform based on β-glucuronidase-selective ABPs to detect and identify subsets of microorganisms in the gut that are responsible for heterologous biological metabolism.[99]

Proteasome inhibitor-based probes

Proteasomes degrade unwanted and damaged proteins, therefore they are the key factor of cellular protein concentration regulation, and the function of the proteasomes is closely related to the development of cancer and neurodegenerative diseases.[100] In 1997, Bogyo and Ploegh developed radioactive ABPs that can label proteasomes.[101] Later, Crews and coworkers developed an ABP by attaching the anti-cancer drug eponemycin with biotin. The proteome study revealed that proteasomes were the main targets of eponemycin.[102] In 2003, Ovaa *et al.* reported a two-step labeling strategy for proteasomes in living cells.[103] By attaching three proteasome subunit inhibitors with different fluorescent groups, the same group reported three proteasome ABPs that target different subunits (**29**, **30** and **31**, Fig. 8A).[104] Using a mixture of the ABPs (ABP-cocktail), they achieved simultaneous gel-based detection of human constitutive core particles (cCP) and immunoproteasome core particles (iCP) proteasomes (β1c, β1i, β2c, β2i, β5c and β5i), which can also be used to distinguish immune cells from non-immune cells.

This work, together with studies of glycosidase ABPs, have shown that sometimes it is possible to derive probes selective for a single enzyme or a small closely related family of enzymes.

Other enzyme inhibitor-based probes

Deubiquitinases (DUBs) are a large group of proteases that catalyze the cleavage of ubiquitin (Ub) from proteins. Due to its important biological functions in the regulation of protein degradation, various ABPs have been developed to study the function of DUBs. In 2016, Tate's team discovered a specific inhibitor of the ubiquitin-specific protease (USP) *via* high-throughput screening. Following this lead, **32** was

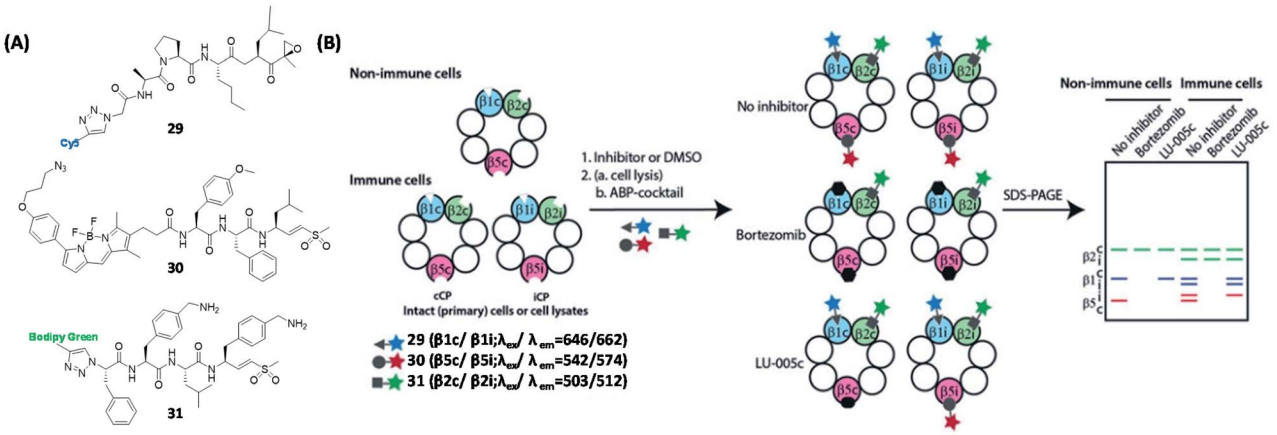

Fig. 8 Inhibitor-based ABPs for labeling of six human proteasome subunits and their working strategies. (A) Structures of ABPs that target different subunits of human proteasomes. (B) Schematic representation of ABPP using proteasome ABP mixture. Visual gel analysis of six human proteasome subunits was achieved using three ABP mixtures. Reproduced from ref. 104 with permission from Wiley-VCH GmbH, copyright 2016.

subsequently designed (Fig. 9A), and shown to be able to identify 12 endogenous USPs from pull-down experiments.[105] Recently, the same group also discovered a specific covalent inhibitor of the ubiquitin carboxy-terminal hydrolase L1 (UCHL1) and subsequently synthesized the corresponding ABP **33** (Fig. 9A).[106] By using proteome profiling, the authors demonstrated that **33** could block the pro-fibrotic response in a cellular model of idiopathic pulmonary fibrosis. Poly (ADP-ribose) polymerase (PARP) is a family of enzymes present in most eukaryotic cells that are involved in multifunctional protein post-translational modification (PTM).[107] Howard *et al.* developed an A*f*BP **34** (Fig. 9A) based on olaparib (a potent inhibitor of PARP1) and showed that **34** could effectively label PARP1/2 in live cells.[108] They also found that **34** enabled successful and selective labeling and inhibition of recombinant PARP6 *in vitro*, therefore providing a potential tool for differentiating PARP6 activities from endogenous sources.

Serine hydrolases play various roles in the regulation of host–pathogen interactions in many organisms.[7] In 2018, Bogyo's group successfully identified 10 previously uncharacterized *S. aureus* serine hydrolases by using competitive ABPP. The new hydrolases were named fluorophosphonate-binding hydrolases (Fph A-J).[109] FphB was selected for the use in the next-stage study due to its overall enzymatic activity in cells and high specificity toward a previously reported inhibitor called JCP251. The authors found that, by substituting the C3 methoxyl group in JCP251 with Bodipy-TMR fluorophore to generate ABP (**35**, Fig. 9A), the resulting probe was able to retain the original inhibitory activity, allowing it to be used as an effective FphB-targeting probe. The proteome reactivity labeling profile of FphB with **35** further showed that FphB activity was mainly concentrated in the separating septum located on the bacterial cell surface (Fig. 9B).

Fatty acid amide hydrolase (FAAH) is an endosomal enzyme that metabolizes many fatty acid amides (FAAs), which are messenger molecules in various living organisms. Severe neurotoxicity was reported in the clinical study of BIA 10-2474 (a FAAH inhibitor). Upon further investigation, Stelt *et al.* revealed that BIA 10-2474's toxicity was caused by its poor target specificity, which resulted in substantial alterations in the human cortical neuron lipid network.[110] To further understand the exact mechanism-of-action that caused BIA 10-2474's toxicity, Cravatt's group employed **36** (Fig. 9A), an ABP designed on the basis of the demethylation metabolite of BIA 10-2474.[111] The authors found **36** was able to irreversibly react with the catalytic Cys present in several aldehyde dehydrogenases, including aldehyde dehydrogenases A2 (ALDHA2). Their findings thus suggested that BIA 10-2474's severe toxicity was possibly caused by the off-target inhibition of this compound as well as its metabolites on these important human enzymes, which are required to properly maintain the physiological stability of the nervous system.

DOT1L is a Lys-methylating enzyme. Overexpression of DOT1L leads to cell cycle arrest, as well as promoting differentiation and apoptosis of tumor cells.[112] For this reason, DOT1L has become an increasingly important therapeutic target for cancer treatment. Based on a potential DOT1L inhibitor, FED1, which showed good *in vitro* inhibitory but poor *in vivo* activity, clickable A*f*BPs, including **37** and **38** (Fig. 9A), were generated to better understand the cellular activity of FED1 in targeting endogenous DOT1L.[113] It was found that **38** displayed higher fluorescence signals in live-cell imaging experiments, whereas **37** showed better performance in most *in vitro* experiments, indicating that the primary amine in the adenine moiety of FED1 may be important for target binding. Further live-cell imaging studies showed that both **37** and **38** were mostly trapped in the cytoplasm of A431 cells and failed to localize to the nucleus where endogenous DOT1L normally resides. These data serve as the basis to potentially explain the relatively poor cellular activities of FED1 and its derivatives, thus providing clues for future improvement of DOT1L inhibitors.

3-Phosphoglycerate dehydrogenase (PHGDH) is an essential enzyme involved in the serine biosynthetic pathway and has been found to be upregulated in numerous rapidly

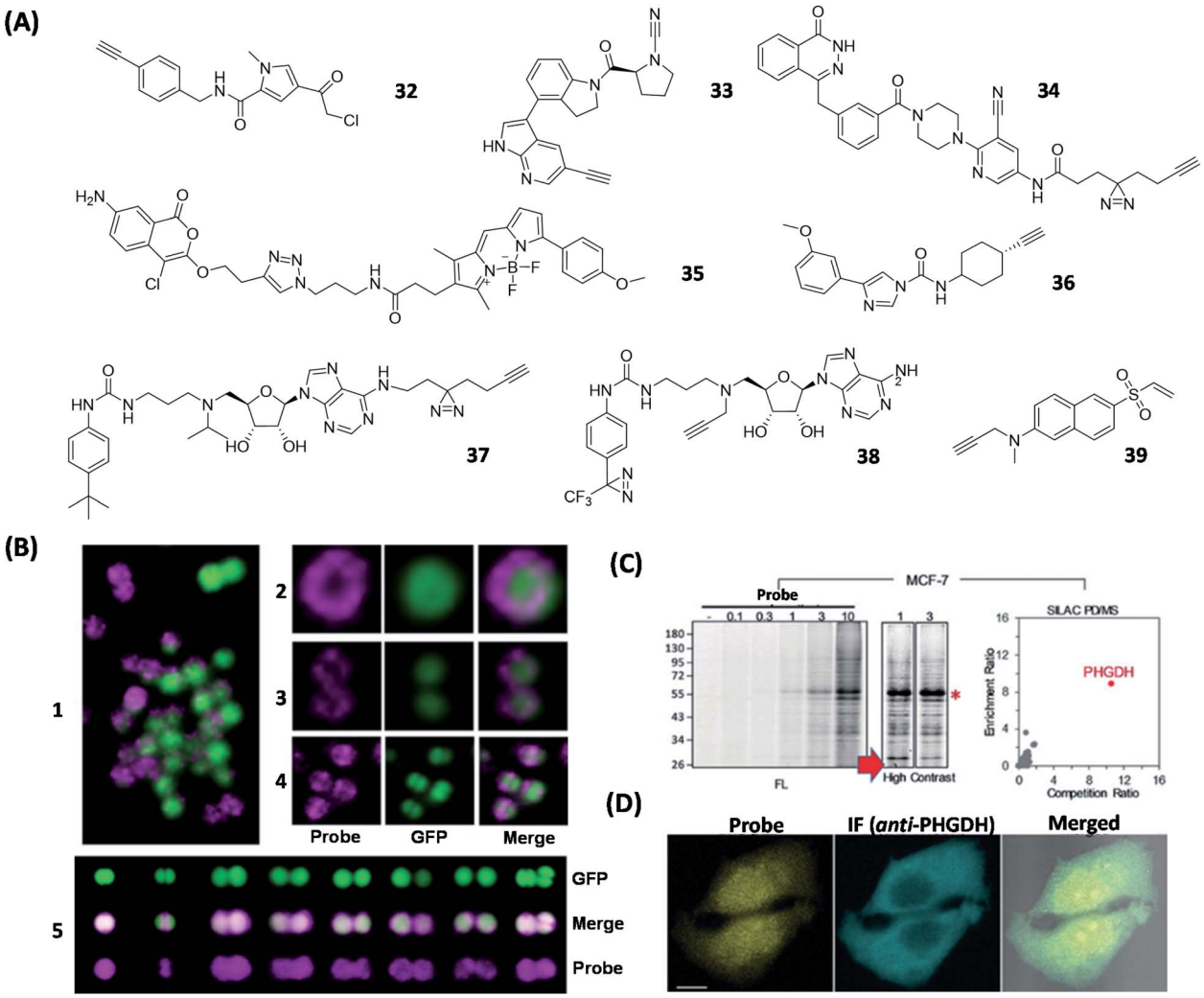

Fig. 9 ABPs and A*f*BPs designed based on specific enzyme inhibitors and their labeling of enzymes in cells. (A) Structures of reported enzyme inhibitor-based ABPs. (B) Confocal images of *S. aureus* Newman labeled with **35** (1). Confocal images of *S. aureus* Newman-GFP cell labeled with **35** during exponential phase (2 and 3) and stationary phase (4 and 5). **35** successfully demonstrated that FphB is concentrated in the isolated membrane of bacterial cells. Reproduced from ref. 109 with permission from Springer Nature, copyright 2018. (C) Proteome profiles of MCF-7 cells labeled with **39**, with a visible FL band around 55 kDa. These demonstrated the specific labeling of PHGDH by **39** in living cells. (D) Confocal images of MCF-7 cells treated with **39** and *anti*-PHGDH. Reproduced from ref. 115 with permission from Wiley-VCH GmbH, copyright 2018.

proliferating cancer cells.[114] In order to develop effective ABPs suitable for *in situ* profiling and live-cell imaging of endogenous PHGDH, molecular docking experiments were first carried out to identify potential small-molecule PHGDH binders. We found that several vinyl sulfone-containing electrophilic phosphotyrosine mimics, including phenyl vinyl sulfone (PVS) and phenyl vinyl sulfonate (PVSN), were well-fitted in the active site of PHGDH, thus presenting a potential electrophilic trap to covalently react with the nearby Cys residue in PHGDH. Further development of these "leads" by taking advantage of the vinyl sulfone's ability to serve as an effective fluorescence quencher,[37] led to the discovery of **39** (Fig. 9A), the first-ever fluorescence Turn-ON ABP that could selectively and covalently label endogenous PHGDH from numerous cancer cells.[115] This dual-purpose probe was able to simultaneously image and profile endogenous enzymatic activities from live mammalian cells (Fig. 9C and D).

Substrate-based ABPs and A*f*BPs for enzymes

In addition to designing ABPs and A*f*BPs based on the inhibitors, another widely used approach employed in the design of enzyme-targeting ABPs and A*f*BPs involves the chemical modification of natural substrates of the target enzymes. These probes have been dominantly used for the biological function studies of enzymes, while inhibitor-based probes are more often used for drug target discovery. Some bifunctional probes that are composed of two binding units could allow rapid enzymatic activity detection and spectroscopic analysis at the same time.

Steviol-based probes

In plants, UDP-glycosyltransferases (UGTs) utilize UDP glucose (UDPG) as a donor to transfer part of the glucose to secondary

metabolites, in an event known as glycosylation.[116] Steviol glycoside (SG) is a natural sweetener biosynthesized from steviol through a series of glycosylation reactions catalyzed by multiple UGTs.[117]

Xiao's group tagged the "minimalist" photo-crosslinker diazine-alkyne to steviol and synthesized a steviol-derived A*f*BP **40** (Fig. 10A) to identify various UGTs involved in steviol catalysis. The proteomic profiling by using **40** confirmed that UGT73E1 was involved in the glycoside biosynthesis of steviol.[118] To improve the selectivity and sensitivity for the identification and labeling of UGTs in biosynthesis, Wong *et al.* developed another method to profile UGTs by using a dual-substrate probe constructed from an alkyne-labeled acceptor **41** and a diazirine-labeled donor **42** (Fig. 10A).[119] Because none of them have the essential properties of the fully functionalized probes, they will not capture the proteins in proteomics experiments. Upon being catalyzed by specific UGTs, the diazirine-modified moiety in donor **42** was transferred to acceptor **41**, thus generating the steviol glycoside-derived probe (Fig. 10B), which, upon subsequent photo-crosslinking, could be used to capture and identify the corresponding UGTs. Using this approach, the authors successfully labeled two glycosyltransferases, UGT73C1 and SrUGT85C2, and showed that both enzymes displayed the same activity against steviol. On the other hand, other UGTs such as SrUGT91D2 and SrUGT76G1, which are involved in steviol glycoside biosynthesis but only catalyze non-steviol glycoside substrates, were not labeled. Compared to previous studies, ABPs generated from this newly developed method showed significantly improved selectivity and sensitivity towards endogenous UGTs.

Furthermore, they found that this modular dual-substrate-probe labeling strategy had an impact on the catalytic efficiency of natural enzymes. By optimizing the probe structure and improving the combination of modules, it may help to broaden the application of the dual-substrate probe labeling strategy for other enzymes.

Nicotinamide adenine dinucleotide (NAD^+)-based probes

Protein ADP-ribosylation is a PTM in which members of the PARP enzymes covalently attach ADP-ribose moieties from NAD^+ to target proteins.[120] PARPs are ADP-ribosylating enzymes that comprise at least 18 members. As the first identified and best-studied PAPR family member, PARP1 regulates a variety of biological functions including DNA repair, chromatin reorganization, transcriptional regulation, apoptosis and mitosis.[121] Under severe and/or continuous stress, PARP1 is activated to promote the synthesis of poly (ADP-ribose) (PAR) chains.[107] The over-activation of PARP leading to rapid depletion of NAD^+ in cells could affect various biological processes. It is therefore necessary to be able to precisely monitor this process in biological cells, preferably in real time. One example is the monitoring and study of the biological functions of NAD^+-associated enzymes by using synthetic NAD^+-based ABPs (Fig. 11). The mechanism of these ABPs is similar to that of NAD^+. First, an ADP-ribosyl group binds to the carboxylate side chain of the substrate protein residues, and the process is then repeated

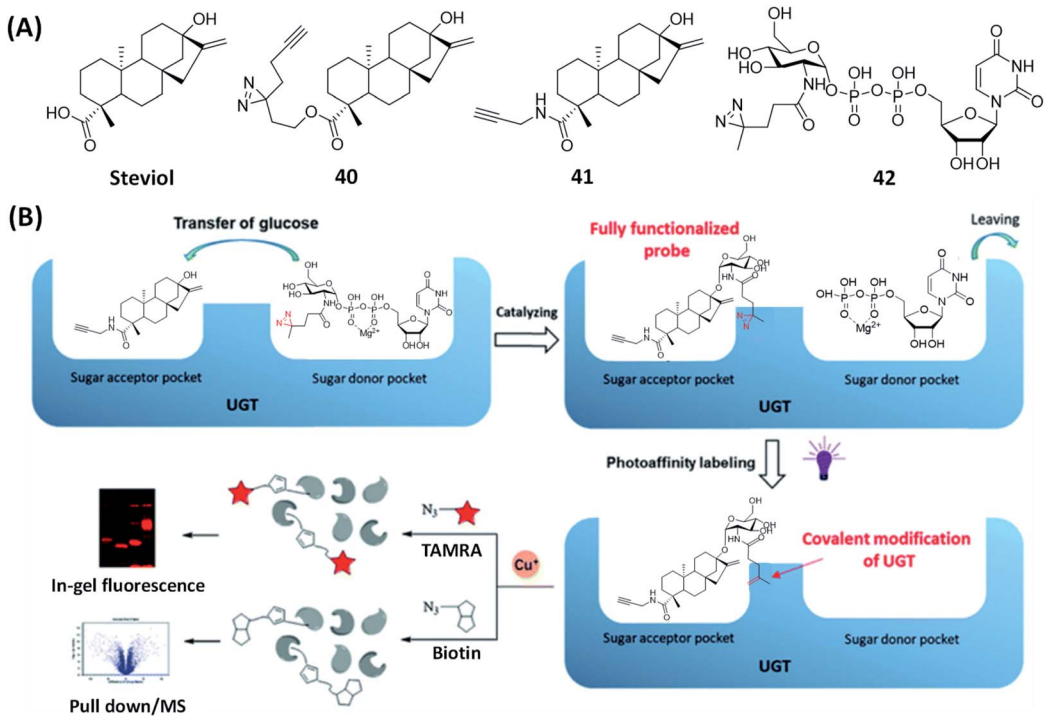

Fig. 10 A bisubstrate probe strategy for specific labeling of UGTs. (A) The structures of steviol and the reported substrate-based ABP and A*f*BPs. (B) Bisubstrate probe strategy for the identification of UGT cellular localization and activities by steviol-based ABPs. Reproduced from ref. 119 with permission from Royal Society of Chemistry, copyright 2020.

with the addition of more ADP-ribosyl groups to the 2′-OH groups of both ribose rings, resulting in the formation of PAR, followed by the enrichment and analysis of PARP substrate proteins by click chemistry. The NAD^+ analogue **43** was successfully synthesized by Jiang *et al.*, and subsequently used to identify 79 proteins as potential PARP1 substrates in a large-scale proteome-wide study.[122] In another study, Buntz *et al.* reported two NAD^+-based ABPs to study protein PARylation.[123] In order to allow PAR activity to be directly monitored *in vivo* and in real-time, the probes were made to be fluorescently active by conjugating them to a fluorophore (tetramethylrhodamine, TMR) (**44**, Fig. 12). SDS-PAGE analysis showed that only **44b** could fluorescently label PARP1 auto-modification. Due to the low cell permeability of NAD^+ analogues, carrier peptide Pep-1 was co-incubated with **44b** to enhance the cellular uptake.[124] Labeling results obtained using flow cytometry demonstrated that more than 90% of the cells were successfully labeled. The formation of PAR in cells was further confirmed by confocal microscopy; a strong fluorescence increase was observed within a few seconds after the induction of DNA damage. Wallrodt *et al.* also synthesized a series of NAD^+ analogues by modifying the adenine moiety at different sites (**45a–d**; Fig. 12);[125] their results indicated that modifications at position 7 (**45d**) and 8 (**45a**) of adenine interfered with the recognition of the probes by their target enzymes. Substitution with a small group at position 6 (**45b**), on the other hand, appeared to be tolerable. Amongst the various probes developed, 2-modified NAD^+ analogues (**45c**, **f**, **g**), which were resistant to chemical modifications (with long and bulky chains), were shown to be the most effective. To explore the function of these probes in live cells, **45g** was taken as a representative to label endogenous PAR from HeLa cells. By further extending the studies on the effects of chemical modification of adenine to other PARPs,[126] the authors showed that 6-modified NAD^+ analogues (**45b**, **b′**) could be reasonably recognized by PARP1/2/5/6, while 2-modified analogues (**45c**, **c′**) exhibited overall better PARP-targeting activities. Further studies revealed that both PARP1 and PAPR2 were able to process 2-modified NAD^+ analogues (**45c**, **c′**), but not the 7- or 8-modified ones (**45d** and **45a**, respectively). Collectively, these studies demonstrated that 2-modified NAD^+ analogues are the best choices in the construction of PAPR1- and PAPR2-specific ABPs. Tankyrases (*e.g.*, PARP5 and PARP6), on the other hand, displayed a preference for 6-modified NAD^+ analogues (**45b**, **b′**), making them preferred choices in future design of ABPs for the study of these PARPs.

Multiple metabolic precursors of NAD^+ (*e.g.*, NR, NA, NAM and NMN) are known to be well-tolerated by numerous human cells to sustain endogenous NAD^+ production,[127] suggesting that it is possible to also metabolically generate NAD^+-based ABPs in live cells that may be used for subsequent proteomic analysis of ADP-ribosylated proteins. With this in mind, Hang *et al.* used a previously reported adenine 6-modified NAD^+ precursor **46** (Fig. 12),[128] and fed it to HeLa cells. Upon successful incorporation into ADP-ribosylated proteins, the authors were able to find that oxidative stress-induced ADP ribosylation of V-Ha-Ras (HRas, a member of Rho GTPases) occurs at the C-terminal hypervariable regions, Cys181 and Cys184.[129] This suggests that not only bacterial toxin, mammalian cells alone were able to regulate the ADP-ribosylation of endogenous GTPases.

Recently, Kalesh *et al.* reported a dual metabolic marker approach for the labeling of substrate proteins in PARylation (Fig. 12).[130] By using ABP **46** and adenine 2-modified NAD^+ precursor ABP **47**, and in combination with tandem mass tag (TMT) isobaric mass spectrometry and hierarchical Bayesian modeling, the authors quantified the response of over a few thousand proteins upon treatment with clinical PARP inhibitors (olaparib and rucaparib).

Different from the aforementioned studies, Zhang *et al.* investigated the effect of substitution at nicotinamide ribose (NR)-OH and synthesized an array of NAD^+ analogues (**48**, Fig. 9).[131] Co-incubation of PARP1 with the NR 3′-OH (**48f**)

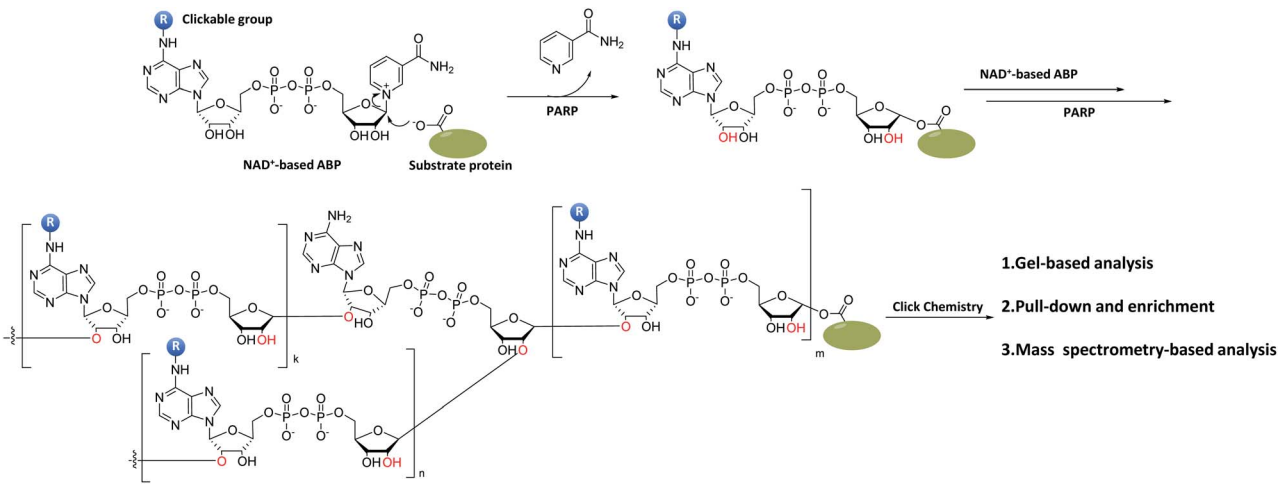

Fig. 11 The mechanism and application of NAD^+-based ABPs (modified adenine moieties as an example). Upon the polyADP-ribosylation *via* PARPs, the PAR is formed from a single ADP-ribosyl linkage on the substrate proteins, which is usually followed by the enrichment and gel-/mass spectrometry-based analysis of PARP substrate proteins through click chemistry.

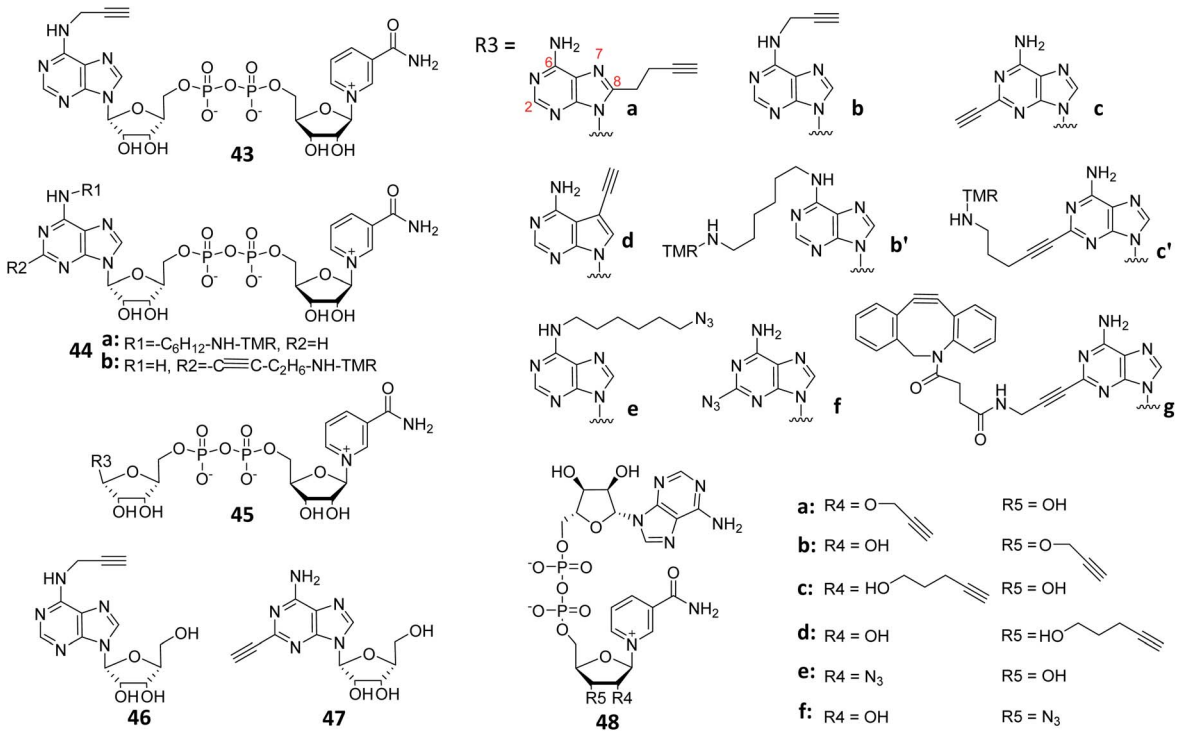

Fig. 12 Structures of reported ABPs based on NAD^+ by modifying adenine or nicotinamide ribose-OH at different sites.

caused a strong auto-PARylation of PARP1, and the addition of veliparib (an inhibitor of PARP1/4) effectively inhibited this process. In contrast, NR 2′-OH analogues (**48a**, **c**, **e**) did not show any substrate activity for PARP1. Meanwhile, **48b** and **48d** exhibited different activities toward PARP1. Kinetic data showed that the K_m of **48f** was slightly higher than that of NAD^+. The K_{cat} of **48b** was significantly lower than those of NAD^+ and **48f**. Successful monitoring of PARylation in living cells was achieved by using **48f** with the assistance of transient permeabilization of cell membranes.[132] When compared to the previously reported adenine-modifying NAD^+ analogues (**45b** and **45c**), **48f** possessed a significantly higher substrate activity against both PARP1 and PARP2 (Fig. 13A and B). Collectively, these results indicate that the NR 3′-OH NAD^+ analogue (**48f**) showed higher activity and selectivity towards PARP1 and PARP2 (Fig. 13C and D).

Cohen's group reported a "bump-hole" strategy, which is an additional method for recognizing the enzymatic target protein of PARP1.[133] This strategy created an orthogonal pair of NAD^+ analogues (**49**, Fig. 14A) and mutated PARP1 by attaching a bulky motif at the nicotinamide of NAD^+ while mutating the "gatekeeper" residue of the PARP1 nicotinamide binding pocket (Fig. 14A), which did not interfere with the normal biological functions of wide-type PARP1. However, this approach diminished the PARylation activity of PARP1 and PARP2, while preserving the MARylation activity. A similar but more elegant strategy was reported in 2016. Instead of modifying the nicotinamide portion, Kraus's team attached an alkyl stalk to the adenine portion of NAD^+ (**50**, Fig. 14B), which served as both a "bump" and a clickable handle for subsequent pull-down experiments (Fig. 14B).[134] They successfully identified hundreds of ADP ribosylation sites for PARP1, PARP2 and PARP3, as well as thousands of PARP1-mediated ADP ribosylation sites using this approach.

Recently, Zhang's group designed and synthesized another series of NAD^+ analogues (**51**, Fig. 15A) containing both diazirine-modified adenine and 3-azide-modified ribose.[135] These bifunctional probes served as good substrates of PARylation and were able to capture PARylation-interacting proteins, including both readers and erasers, *via* PAL (Fig. 15B). With probe **51c** alone, the authors were able to capture up to 247 possible interacting proteins from cell lysates.

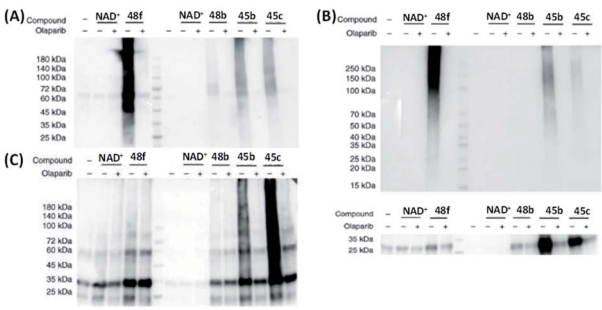

Fig. 13 Gel-based analysis of substrate activities of NAD^+, **48b**, **f** and **45b**, **c** for (A) PARP1; (B) PARP2; (C) catalytic domain of PARP5a; and (D) catalytic domain of PARP10. All the probes were successfully recognized by the corresponding enzymes, and the addition of PARP inhibitor olaparib efficiently inhibited the interactions between the probes and PARPs. Reproduced from ref. 131 with permission from Springer Nature, copyright 2019.

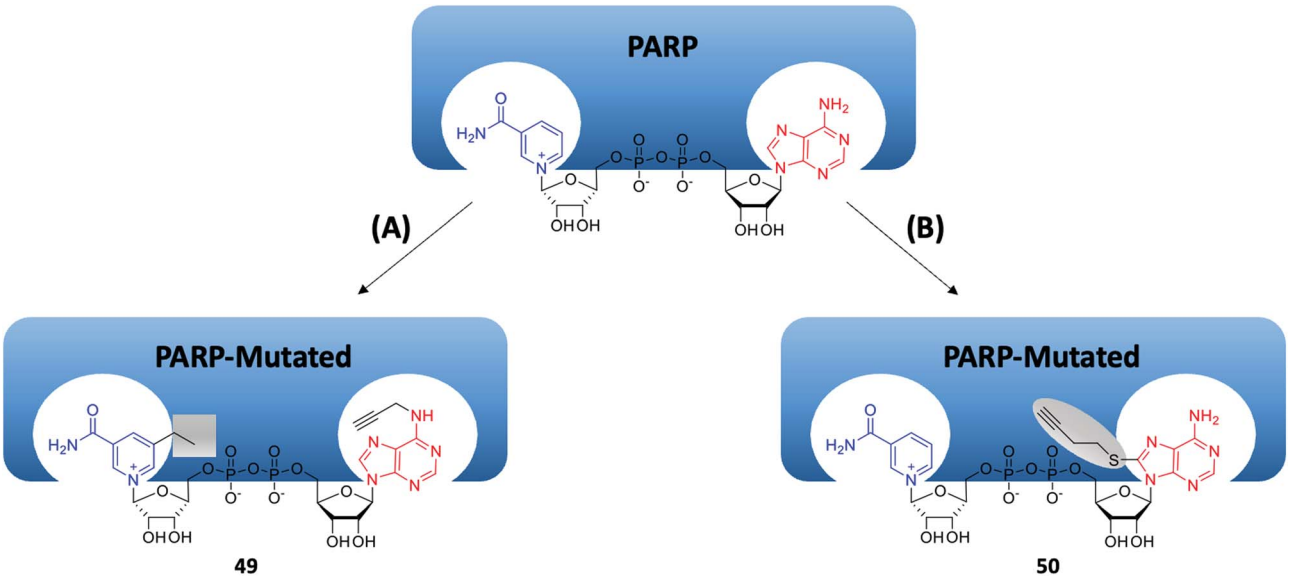

Fig. 14 Two approaches of the "bump-hole" strategy for identifying PARP target proteins. (A) Targeting a conserved residue in the nicotinamide binding site of the PARP catalytic domain. (B) Targeting a conserved residue in the adenine binding site of the PARP catalytic domain.

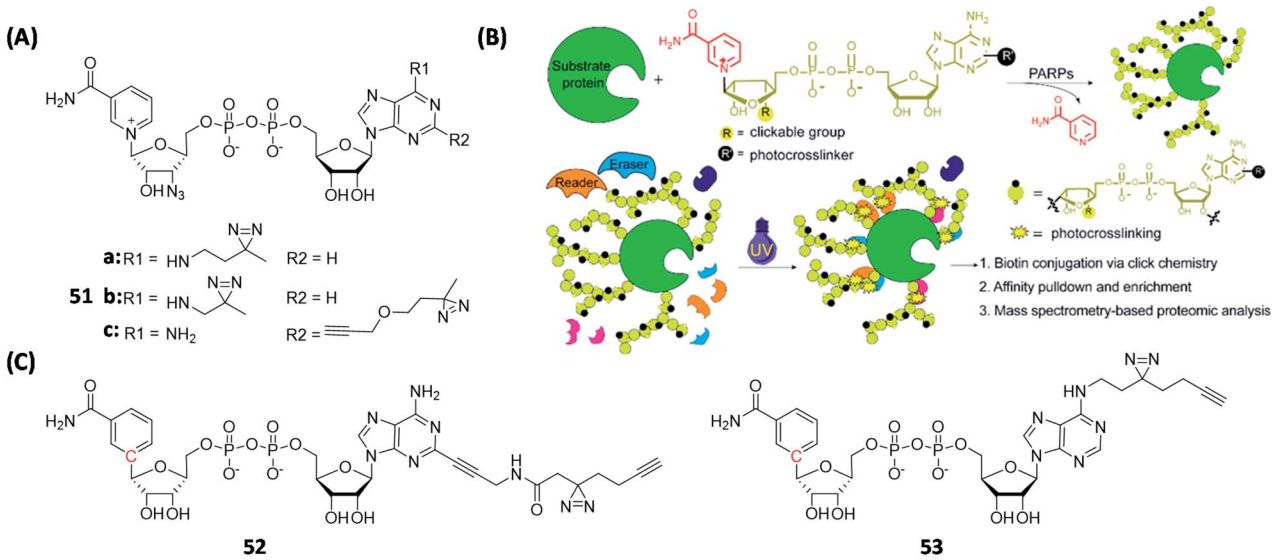

Fig. 15 Use clickable A*f*BPs to capture proteins associated with PARylation. (A) Structures of reported bifunctional NAD^+ probes. (B) Schematic illustration of the process for capturing PARylation-related interacting proteins using a bifunctional NAD^+ probe. Reproduced from ref. 135 with permission from American Chemical Society, copyright 2021. (C) Structures of reported BAD-based clickable A*f*BPs.

Among these proteins, VCP and RBBP7 were selected for further biological validations; in ELISA-binding assays and immunoblotting experiments, both VCP and RBBP7 were shown to specifically interact with PARP1. Using a similar strategy, Cohen's group developed clickable A*f*BPs (**52** and **53**, Fig. 15C) based on benzamide adenine dinucleotide (BAD, another NAD^+ analogue).[136] They identified hundreds of both known and unknown NAD^+/NADH binding proteins by using **52** and **53** (261 and 141 proteins were identified from the **52**- and **53**-treated samples, respectively), which primarily labeled different proteins but also share some common targets. These clickable NAD^+-based A*f*BPs provide new tools for analyzing proteins that interact with NAD^+ in different diseases.

Ubiquitin (Ub)-based probes

Ubiquitination is an important reversible PTM in eukaryotic cells. It plays important roles in protein localization, metabolism, function, regulation, and degradation.[137] Ubiquitination occurs *via* a three-enzyme-catalyzed reaction which involves E1, E2 and E3 proteins. Ub molecules can be coupled to other Ubs to form poly-Ub chains. By hydrolyzing the isopeptide linkage in ubiquitinated proteins, DUBs remove Ub molecules from their

substrates as well as Ub-processing precursors.[138] Therefore, Ub-based ABPs and AfBPs are effective tools to monitor the biological functions of key enzymes that are involved in the ubiquitination cycle.

Most of the probes used in the characterization of DUBs were designed on the basis of mono- or diUb. Since most DUBs have active Cys residues in their catalytic centers, most reported Ub-based probes contain a thiol-reactive functional group (*e.g.* a Michael acceptor) that allows for covalent reactions with the Cys residues in DUBs. Strictly speaking, such probes may be considered "inhibitors", but we simply group them herein as "substrate-based ABPs" for convenience, as all of them were derived from natural substrates of DUBs (*i.e.* Ub).

DUBs employ multiple Ub-binding pockets to break down polyubiquitin (poly-Ub) chains. Ovaa's team reported a series of non-hydrolyzable protease-resistant diUb ABPs (*i.e.* **54**, Fig. 16A)[139] for the identification and investigation of specific linkage reactions of DUBs with diverse Ub-binding pockets. These probes covered seven different linkage positions (connected at seven Lys positions of Ub, *i.e.* K6/K11/K27/K29/K33/K48/K63) and contained protease-resistant triazole bonds as well as a propargyl group at the C-terminus of the adjacent Ub part. *In vitro* DUB cleavage experiments were used to determine the linkage specificity of the S2 pocket in DUBs. Results showed that OTUD2 was conjugated with K11- and K33-linked diUb, and OTUD3 was bonded with K11-linked diUb in the S1–S2 pocket. Whedon *et al.* developed two selenoCys (SeCys)-based approaches to introduce DUB-reactive dehydroalanine (DHA) at the C-terminus of Ub.[140] Through efficient oxidation or alkylative β-elimination of SeCys, DHA could be selectively conjugated at the C-terminus of Ub where several Cys residues in the target of Ub were present. ABP **55** was designed to target TRIM-25, an E3 ligase tripartite sequencing protein (Fig. 16A). Upon positive interaction between **55** and DUBs, the Cys sulfhydryl group in **55** formed a covalent bond through DHA with the active site of DUBs. The captured DUBs were next identified in a pull-down experiment. These so-called alkylation–elimination DUB-targeting strategies effectively resolved the interference of other Cys residues in the target of Ub, thus providing new chemical biology tools for future design of novel DUB ABPs.

Liang *et al.* reported two diUb-based AfBPs, **56** and **57** (Fig. 16A), which were able to selectively analyze ubiquitin-binding proteins from cell lysates.[141] Different Ub–Ub linkages were found to exhibit practical variations. For example, Lys63-conjugated poly-Ub was the signal for transduction.[142] Based on this knowledge, the diUb core in the two designed AfBPs (*i.e.* **56** and **57**) were conjugated *via* Lys48 and Lys63 linkage, respectively, resulting in probes that exhibited different protein selection preferences. In addition, the Ala46 residues of two Ub units were mutated to Cys, which was then attached to photo-crosslinkers including diazine and aryl-azide. With such probes, the authors discovered that at least two Ub units were required to efficiently capture Ub-binding proteins *via* PAL.

Meledin *et al.* constructed a ubiquitinated α-globin ABP (**58**, Fig. 16A), through a semisynthetic strategy based on sequential DHA formation on the expressed proteins.[143] α-Globin can be ubiquitinated at multiple sites to facilitate their proteasomal degradation.[144] By using large-scale proteomic analysis, the authors discovered that USP15 acted as a potential DUB for the regulation of α-globin, and overexpression of UPS15 exacerbated the thalassemia symptoms.

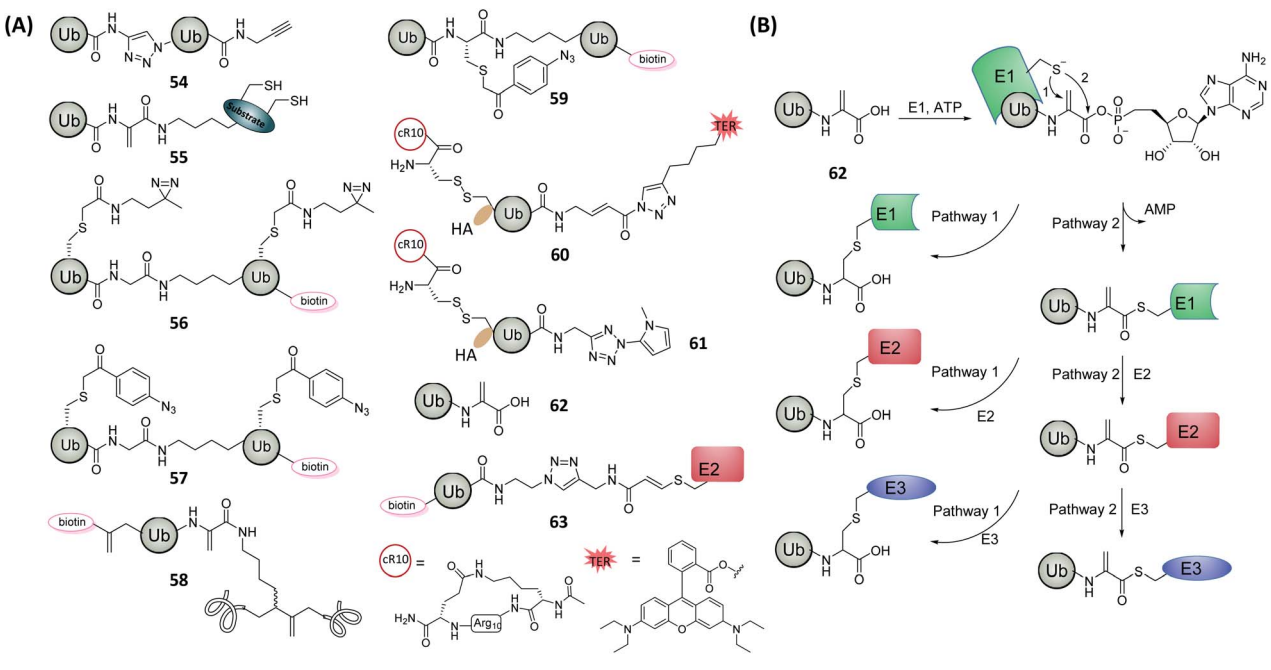

Fig. 16 Ub-based ABPs and AfBPs for DUBs and E1, E2, E3 enzyme studies. (A) Structures of reported ABPs and AfBPs based on Ub. (B) Mechanism of **62** for the labeling of E1, E2 and E3 enzymes. Pathway (1): enzymatic covalent binding process, pathway (2): natural *trans*–*trans* thioesterification process.

The Lys27-linked poly-Ub plays a vital role in autoimmunity and DNA repair.[145] Based on previous studies,[141,146] Tan *et al.* reported a diUb probe **59** (Fig. 16A) for the identification of DUBs that regulate the synthesis and degradation of K27-linked poly-Ub.[147] The probe carried an aryl-azide group as the photo-crosslinker at the isopeptide position, and a biotin tag was attached to the C-terminus of the probe. When compared with the earlier-discussed, DHA-based probes,[140,143] **59** exhibited higher crosslinking activity for Lys27-linkage-targeting DUBs. Pull-down experiments demonstrated that the probes could recognize K27-targeting DUBs present in the crude proteome, a key property which was not possible with earlier DHA-based probes.

Most Ub-based DUB-targeting ABPs, however, had poor cell permeability due to their macromolecular nature. This has severely limited their *in cellulo* and *in vivo* applications. In 2018, Zhuang's group reported a cell-permeable DUB-targeting ABP (**60**, Fig. 16A) that enabled intracellular DUB profiling.[148] An HA tag and a cyclic polyarginine (cR10) peptide were conjugated to Ub *via* a disulfide bond, the HA tag was then attached to the N-terminus of the probe. As a cell-permeabilizing peptide, cR10 enabled the cellular uptake of **60**, which was then removed from the probe upon successful cell entry and subsequent disulfide bond cleavage caused by endogenous GSH.[149] **60** was successfully used to monitor endogenous DUBs present in various organelles by fluorescence imaging.

Recently, a tetrazole group which is a new type of photo-crosslinker,[150] was attached to the C-terminus of Ub, producing probe **61** (Fig. 16A).[151] This probe successfully pulled down and identified fifteen known DUBs, and upon further optimizations, the probe was used to identify specific DUBs proteomes in cells that were grown during G1/S and G2/M phases. By comparing enriched DUBs from the two cell growth phases, five DUBs in G1 phase and one DUB in G2 phase were specifically identified, respectively. Amongst them, BAP1 and USP36 were closely related to the regulation of ubiquitination in the G1 phase as reported previously.[152] The doubly enriched DUB USP16, previously known to have a function in regulating protein localization in the G2 phase,[153] was also discovered. Using a time-gradient identification assay, the function of this DUB during cell mitosis was further demonstrated.

Mulder *et al.* developed a cascading ABP **62** (Fig. 16A),[154] based on a previous study that the mutation Ub-G76A still retained the ability of being processed through the E1–E2–E3 cascade.[155] With this knowledge, the authors hypothesized that partial replacement of this C-terminal Ala of this Ub mutant further with the electrophilic DHA (giving **62**) may also preserve the activity of Ub (Fig. 16B). Indeed, **62** was found to be conjugated to the corresponding enzyme in each step during the E1–E2–E3 cascade reaction by two different ways either forming thioether adducts by covalently binding to enzymes (pathway 1), or generating thioester compounds with enzymes *via* the natural linkage pathway (pathway 2). Therefore, **62** was an excellent ABP that could be used in the study of each step in the E1–E2–E3 cascade reaction.

Virdee's team deduced that the E2–Ub complex could serve as a starting substrate for the analysis of *trans*-thiolation activities in E3 ligases, *i.e.* RING-in-between-RING (RBR) and homologous to E6AP carboxy-terminus (HECT). Therefore, ABP **63** (Fig. 16A) was prepared as a non-hydrolytic mimic of E2–Ub, in which the unstable thioester bond was suitably stabilized. An appropriate and dynamically tuned electrophilic reagent was further installed between Ub and E2 as well.[156] The resulting **63** was able to successfully monitor the *trans*-thiolation activity of parkin (a RBR E3 ligase) *in vitro* from cell lysates, thereby providing a potential tool to directly and quantitatively detect endogenous parkin activity. With the same strategy, the authors were able to further identify that the neural-associated E3 ligase, MYCBP2 (PHR1), was a novel class of cyclic E3 ligases capable of selective esterification of Thr over Ser in their substrates.

Other substrate-based probes

For enzymes that lack effective ABPs or A*f*BPs, rational substrate design or high-throughput screening may generate effective initial leads for subsequent construction of specific chemical probes. Moreover, by modifying existing enzyme-targeting probes with different functional groups while retaining their enzyme specificity, some probes may be repurposed that enable simultaneous single-step fluorescence-based enzyme detection and proteome-wide profiling.

Histone deacetylases (HDACs) are a class of enzymes that play an imperative part in the structural modification of chromosomes and in gene expression regulations.[157] In 2016, Sun's group combined a simple HDAC substrate, *e.g.* the acylated Lys (Kac), with a fluorogenic dye, *O*-NBD, to develop the corresponding activity-based fluorescence Turn-ON probe **64** (Fig. 17A).[158] Upon enzymatic cleavage of Kac in the probe by HDAC, the resulting uncaged Lys intramolecularly attacked the *O*-NBD moiety, subsequently turning on the probe fluorescence. The enhanced fluorescence intensity was shown to be up to 50 folds, which made probe **64** an excellent HDAC-based fluorogenic ABP. Based on these results, the authors further introduced a diazirine-alkyne photo-crosslinker group into the probe, generating a dual-purpose fluorescent probe **65** (Fig. 17A). The probe **65** was shown to not only function as a fluorogenic substrate probe, but also recognize and capture target proteins from cell lysates. By combining fluorescence assays and in-gel fluorescence scanning, **65** successfully identified and differentiated epigenetic readers BRD4-1 and erasers Sirt2 (Fig. 17B).

Lys lipoylation (Klip) is a conserved Lys PTM, and plays an important role in the regulation of cellular metabolism.[159] K105 ($QSDK_{lip}ASVT$) is a peptide sequence of the branched-chain α-ketoacid dehydrogenase (BCKDH), which is one of several metabolic multi-complexes where Klip is known to occur.[160] By utilizing a similar strategy as in the design of the earlier-discussed HDAC probe, the same group developed an A*f*BP **66** (Fig. 17C), which was based on the peptide sequence $QSDK_{lip}$-ASVT with replacement of the N-terminal Gln residue with a photo-crosslinker.[161] Gel-based profiling and pull-down experiments demonstrated that Sirt2 (an NAD^+-dependent deacetylase) caused significant delipoylation of **66**. To further investigate the potential activity of Sirt2 on Klip, a fluorogenic probe with *O*-NBD group that can detect delipoylation activity in

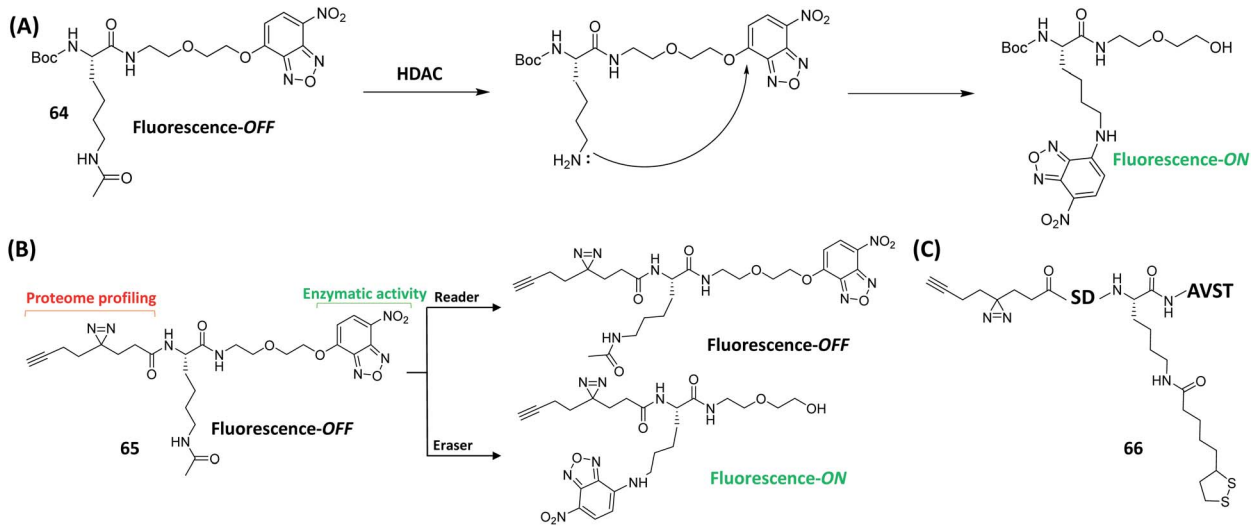

Fig. 17 Single-step fluorescence detection and identification of enzyme readers and erasers using A*f*BPs. (A) Schematic of HDAC detection using fluorometric method. (B) Schematic illustration of **65** for detecting enzymatic activity and proteomic profiling studies. Single-step fluorescence detection and proteomic profiling of HDAC can be achieved simultaneously by using **65**. (C) Structure of A*f*BP **66** for the identification of Klip erasers.

a single step was next developed. The following kinetic data demonstrated that Sirt2 had a strong delipoylation capacity *in vitro*, even better than that of Sirt 4, previously the only identified mammalian delipidylase. These innovative findings thus suggest that sirtuins may regulate cellular Klip through different delipoylation mechanisms.

Methylation events in various organisms are essential for the regulation of DNA transcription, RNA stability, and protein activity.[162,163] They are catalyzed by a host of methyltransferases in cells. Among them, the *S*-adenosine methionine (SAM)-dependent methyltransferases (MTs), capable of transferring a methyl group from SAM to their biological substrates, are the most prominent class in methylation.[164] The resulting metabolite byproduct of this reaction, *S*-adenosyl-*L*-homoCys (SAH), may be further metabolized to methione (an amino acid) which is then reintegrated into SAM biosynthesis.[165] Inspired from previous work of Dalhoff *et al.*,[166] and crystallographic data of SAM- and SAH-binding enzymes, Cravatt's group functionalized the *N*-6 position of SAH with different linkers to generate a series of SAH-based A*f*BPs (**67**, Fig. 18A).[167] Among them, **67b** was used in the analysis and enrichment of a large number of endogenous MTs from the lysates of human cancer cells (Fig. 18B), with excellent selectivity over other classes of proteins.

Forward genetics starts with a phenotype which subsequently leads to the identification of interesting genotypes, while reverse genetics starts with a known genotype and finally ends up with various phenotypes.[168] The various aforementioned substrate/ligand screening strategies fit in the field of reverse genetics, but due to the limited size of available chemical libraries, their results are not always optimal. Cravatt *et al.* recently applied the concept of forward genetics in their screening of ABPs by incubating probes that contain covalent binding WHs and click handles with whole-cell proteome.[31,169,170] Therefore, the pulled-down proteins were the

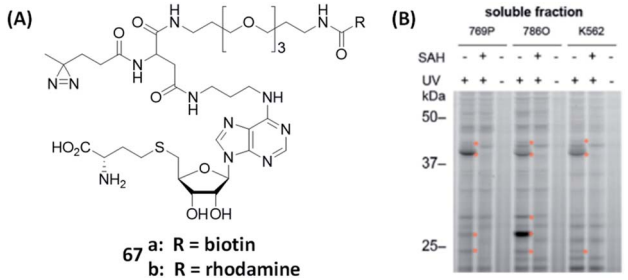

Fig. 18 Gel-based analysis of MTs was performed using A*f*BPs. (A) Structures of reported A*f*BPs for MTs. (B) Gel-based profiling with **67b** in human renal cancer cell (769P and 786O) and human leukemia cell (K562) lysates. **67** successfully labeled MTs in a variety of cancer cells. The addition of SAH (natural substrate) or the lack of UV irradiation resulted in the loss of MT labeling. Reproduced from ref. 167 with permission from American Chemical Society, copyright 2019.

target proteins of the probes. Furthermore, due to the ease of synthesis, it is relatively less complicated to form a small probe library. By using forward genetic screening of the probe library with the whole proteome, the authors confirmed that rapid discovery of ABPs that possess high selectivity against specific sets of enzymes could be realized.

Conclusions and outlook

As an emerging technological approach in the field of chemical proteomics, ABPP is a powerful tool that enables unbiased and quantitative detection of enzymatic activity by measuring cellular and tissue profiles, thereby allowing researchers to gain insights into the functional state of an enzyme rather than only its abundance.

The use of ABPs and A*f*BPs is critical in ABPP. The main enzymes for which ABPs or A*f*BPs have been developed and are

available including kinases, proteases, glycosidases, phosphatases and oxidoreductases. The successful application of ABPP *in cellulo* and animal models has identified a range of enzymatic activities associated with diseases that are closely related to each other. In addition, the development of these probes and ABPP has facilitated functional studies of enzymes involved in many biological processes, including neurotransmission, neurodegenerative diseases, signal transduction in tumors and immune diseases. All these events demonstrate the important role of ABPs and A*f*BPs in the discovery and study of enzyme function. In this review, we have summarized design strategies of different ABPs and A*f*BPs. Inhibitor-based probes have been widely used to identify off-targets, thereby aiding drug discovery and optimization. Substrate-based probes are favorable tools for enzyme functional studies and substrate discovery. The discovery of drug targets is one of the important tasks in the initial studies of clinical drugs. In addition, most of the current proteomics platforms are only able to capture enzymes in a small fraction of samples of cells and tissues. It is still challenging to apply ABPP to routine biological systems. In addition, non-specific labeling of probes and inefficient PAL remain a great challenge. The emergence of various new photo-crosslinkers and the development of bioorthogonal chemistry in recent years have provided some assistance for this purpose. How to obtain high PAL efficiency while reducing the impact of biological systems is also an issue to be addressed in the design of ABPs and A*f*BPs.

The visualization of important enzymatic activity could also be achieved by using highly selective fluorescent ABPs or A*f*BPs. For instance, Shrivastav *et al.* developed a near-infrared fluorescence (NIRF) ABP that was capable of imaging large polyps using a dual-laser NIRF endoscope.[171] Recent years have seen a dramatic increase in the number of near-infrared region II (NIR-II) fluorescent molecules being used in a wide range of bioimaging and biosensing applications.[172,173] The introduction of NIR-II dyes into the fabrication of ABPs and A*f*BPs could potentially expand their applications to disease diagnosis, surgical resection, and therapeutic response validation. Such novel ABPP strategies could offer new opportunities in interdisciplinary research collaborations.

However, due to the complexity and diversity of enzymes, ABPP still faces several issues such as poor specificity and sensitivity. For example, no ABP that can label inverting glycosidases has been reported, but A*f*BPs that were reported by Stubbs *et al.* successfully labeled them.[174] This opens up the possibility of targeting other enzyme families that do not have nucleophilic residues and cannot be labeled by ABPs. In addition, most human enzymes lack selective chemical ligands and some classes of proteins are even considered undruggable. Therefore, it is difficult to develop probes to study these proteins.[170] To overcome such problems, tremendous efforts have been put into the development of more advanced probe design strategies. Bump-and-hole strategy is one solution. By attaching one bulky group at the natural substrate, and at the same time mutating the "gatekeeper" residue of the substrate binding pocket of the enzyme, the orthogonal pair of the probe and the mutated enzyme is formed. Using this orthogonal "bump-hole" system, the specific target proteins of the corresponding enzyme can be identified. This method was successfully used in the ABPP of PARP and Ub.[134,136,141] Bump-and-hole is a powerful method but this chemical genetic approach is limited to *in cellulo* studies, and is less utilized in the ABPP studies of other enzymes. Another approach, has isoTOP-ABPP, developed by Cravatt's group,[29] which uses isotope-labeled probes to obtain more reliable results than other quantitative protein analysis methods. They have also developed fluoPol-ABPP[30] that could be used in combination with HTS to discover new protein ligands. RP-ABPP,[31] an unbiased method which employs nucleophilic hydrazine probes to capture active protein-bound electrophiles in cells,[175] was also developed by the same group. High-throughput forward genetic screening of the whole proteome is another effective method that has been used in the discovery of highly selective chemical probes capable of targeting less-studied enzymes.[169]

In summary, ABPP is a multidisciplinary technology involving chemistry, biology, medicine and other disciplines. There is no single design strategy that is a universal remedy for all research needs. The design and development of better ABPs and A*f*BPs also require interdisciplinary efforts. We hope that this review will contribute to the design and development of more powerful ABPs and A*f*BPs to facilitate further advancement in the research of enzymes.

Author contributions

H. F., B. P., L. L. and S. Q. Y. presented the outline of this review. H. F. wrote the draft. H. F. and B. P. performed the graphic design. O. S. Y., Q. W., L. L. and S. Q. Y. revised and edited the draft. B. P., L. L., and S. Q. Y. conceived and supervised this project. All authors participated in the discussion of the draft and carefully revised the draft before the final submission.

Conflicts of interest

There are no conflicts to declare.

Acknowledgements

This work was financially supported by GSK-EDB Trust Fund (R-143-000-88-592), the Synthetic Biology Research & Development Programme (SBP) of National Research Foundation (SBP-P4 and SBP-P8) of Singapore, the National Key R&D Program of China (2020YFA0709900), the National Natural Science Foundation of China (22077101, 22004099), the Joint Research Funds of Department of Science & Technology of Shaanxi Province and Northwestern Polytechnical University (2020GXLH-Z-008, 2020GXLH-Z-021 and 2020GXLH-Z-023), the Natural Science Foundation of Ningbo (202003N4049, 202003N4065), the Open Project Program of the Analytical & Testing Center of Northwestern Polytechnical University (2020T018), the Open Project Program of Wuhan National Laboratory for Optoelectronics (No. 2020WNLOKF023), Key Research and Development Program of Shaanxi (2020ZDLGY13-04, 2021KW-49), China-

Sweden Joint Mobility Project (51811530018) and Fundamental Research Funds for the Central Universities.

Notes and references

1 U. Markel, K. D. Essani, V. Besirlioglu, J. Schiffels, W. R. Streit and U. Schwaneberg, *Chem. Soc. Rev.*, 2020, **49**, 233–262.
2 R. H. Wijdeven, J. Neefjes and H. Ovaa, *Trends Cell Biol.*, 2014, **24**, 751–760.
3 M. Uttamchandani, C. H. Lu and S. Q. Yao, *Acc. Chem. Res.*, 2009, **42**, 1183–1192.
4 M. J. Evans and B. F. Cravatt, *Chem. Rev.*, 2006, **106**, 3279–3301.
5 L. E. Sanman and M. Bogyo, *Annu. Rev. Biochem.*, 2014, **83**, 249–273.
6 M. J. Niphakis and B. F. Cravatt, *Annu. Rev. Biochem.*, 2014, **83**, 341–377.
7 Y. Liu, M. P. Patricelli and B. F. Cravatt, *Proc. Natl. Acad. Sci. U. S. A.*, 1999, **96**, 14694–14699.
8 D. Greenbaum, K. F. Medzihradszky, A. Burlingame and M. Bogyo, *Chem. Biol.*, 2000, **7**, 569–581.
9 Y. Su, J. Ge, B. Zhu, Y. G. Zheng, Q. Zhu and S. Q. Yao, *Curr. Opin. Chem. Biol.*, 2013, **17**, 768–775.
10 S. Pan, H. Zhang, C. Wang, S. C. Yao and S. Q. Yao, *Nat. Prod. Rep.*, 2016, **33**, 612–620.
11 E. M. Sletten and C. R. Bertozzi, *Acc. Chem. Res.*, 2011, **44**, 666–676.
12 K. Lang and J. W. Chin, *Chem. Rev.*, 2014, **114**, 4764–4806.
13 V. V. Rostovtsev, L. G. Green, V. V. Fokin and K. B. Sharpless, *Angew. Chem., Int. Ed.*, 2002, **41**, 2596.
14 J. C. Jewett, E. M. Sletten and C. R. Bertozzi, *J. Am. Chem. Soc.*, 2010, **132**, 3688–3690.
15 M. L. Blackman, M. Royzen and J. M. Fox, *J. Am. Chem. Soc.*, 2008, **130**, 13518–13519.
16 A. Singh, E. R. Thornton and F. H. Westheimer, *J. Biol. Chem.*, 1962, **237**, 3006–3008.
17 H. Shi, C. J. Zhang, G. Y. Chen and S. Q. Yao, *J. Am. Chem. Soc.*, 2012, **134**, 3001–3014.
18 F. Ragaini, A. Penoni, E. Gallo, S. Tollari, C. Li Gotti, M. Lapadula, E. Mangioni and S. Cenini, *Chem.–Asian J.*, 2003, **9**, 249–259.
19 A. Saghatelian, N. Jessani, A. Joseph, M. Humphrey and B. F. Cravatt, *Proc. Natl. Acad. Sci. U. S. A.*, 2004, **101**, 10000–10005.
20 G. L. Chee, J. C. Yalowich, A. Bodner, X. Wu and B. B. Hasinoff, *Bioorg. Med. Chem.*, 2010, **18**, 830–838.
21 Z. Li, L. Qian, L. Li, J. C. Bernhammer, H. V. Huynh, J. S. Lee and S. Q. Yao, *Angew. Chem., Int. Ed.*, 2016, **55**, 3254.
22 J. Xu, X. Li, K. Ding and Z. Li, *Chem.–Asian J.*, 2019, **15**, 34–41.
23 E. Smith and I. Collins, *Future Med. Chem.*, 2015, **7**, 159–183.
24 W. Lang, C. Yuan, B. Zhu, S. Pan, J. Liu, J. Luo, S. Nie, Q. Zhu, J. S. Lee and J. Ge, *Org. Biomol. Chem.*, 2019, **17**, 3010–3017.
25 C. Guo, Y. Chang, X. Wang, C. Zhang, P. Hao, K. Ding and Z. Li, *Chem. Commun.*, 2019, **55**, 834–837.
26 H. Zhang, R. Liu, J. Liu, L. Li, P. Wang, S. Q. Yao, Z. Xu and H. Sun, *Chem. Sci.*, 2016, **7**, 256–260.
27 Z. Li, D. Wang, L. Li, S. Pan, Z. Na, C. Y. Tan and S. Q. Yao, *J. Am. Chem. Soc.*, 2014, **136**, 9990–9998.
28 Z. Q. Li, P. L. Hao, L. Li, C. Y. J. Tan, X. M. Cheng, G. Y. J. Chen, S. K. Sze, H. M. Shen and S. Q. Yao, *Angew. Chem., Int. Ed.*, 2013, **52**, 8551–8556.
29 E. Weerapana, C. Wang, G. M. Simon, F. Richter, S. Khare, M. B. D. Dillon, D. A. Bachovchin, K. Mowen, D. Baker and B. F. Cravatt, *Nature*, 2010, **468**, 790–795.
30 D. A. Bachovchin, S. J. Brown, H. Rosen and B. F. Cravatt, *Nat. Biotechnol.*, 2009, **27**, 387–394.
31 M. L. Matthews, L. He, B. D. Horning, E. J. Olson, B. E. Correia, J. R. Yates, P. E. Dawson and B. F. Cravatt, *Nat. Chem.*, 2017, **9**, 234–243.
32 G. Blum, G. von Degenfeld, M. J. Merchant, H. M. Blau and M. Bogyo, *Nat. Chem. Biol.*, 2007, **3**, 668–677.
33 L. Qian, L. Li and S. Q. Yao, *Acc. Chem. Res.*, 2016, **49**, 626–634.
34 F. V. Filipp, *Canc. Metastasis Rev.*, 2017, **36**, 91–108.
35 B. R. Lannine, L. R. Whitby, M. M. Dix, J. Douhan, A. M. Gilbert, E. C. Hett, T. Johnson, C. Joslynl, J. C. Kath, S. Niessen, L. R. Roberts, M. E. Schnute, C. Wang, J. J. Hulce, B. X. Wei, L. O. Whiteley, M. M. Hayward and B. F. Cravatt, *Nat. Chem. Biol.*, 2014, **10**, 760–767.
36 H. Fu, H. Fang, J. Sun, H. Wang, A. Liu, J. Sun and Z. Wu, *Curr. Med. Chem.*, 2014, **21**, 3271–3280.
37 N. Berndt, R. M. Karim and E. Schonbrunn, *Curr. Opin. Chem. Biol.*, 2017, **39**, 126–132.
38 J. A. Woyach, E. Bojnik, A. S. Ruppert, M. R. Stefanovski, V. M. Goettl, K. A. Smucker, L. L. Smith, J. A. Dubovsky, W. H. Towns, J. MacMurray, B. K. Harrington, M. E. Davis, S. Gobessi, L. Laurenti, B. Y. Chang, J. J. Buggy, D. G. Efremov, J. C. Byrd and A. J. Johnson, *Blood*, 2014, **123**, 1207–1213.
39 J. C. Byrd, R. R. Furman, S. E. Coutre, I. W. Flinn, J. A. Burger, K. A. Blum, B. Grant, J. P. Sharman, M. Coleman, W. G. Wierda, J. A. Jones, W. Q. Zhao, N. A. Heerema, A. J. Johnson, J. Sukbuntherng, B. Y. Chang, F. Clow, E. Hedrick, J. J. Buggy, D. F. James and S. O'Brien, *N. Engl. J. Med.*, 2013, **369**, 32–42.
40 J. Chen, X. Wang, F. He and Z. Pan, *Bioconjugate Chem.*, 2018, **29**, 1640–1645.
41 X. Wang, N. Ma, R. Wu, K. Ding and Z. Li, *Chem. Commun.*, 2019, **55**, 3473–3476.
42 S. Kobayashi, T. J. Boggon, T. Dayaram, P. A. Janne, O. Kocher, M. Meyerson, B. E. Johnson, M. J. Eck, D. G. Tenen and B. Halmos, *N. Engl. J. Med.*, 2005, **352**, 786–792.
43 S. Planken, D. C. Behenna, S. K. Nair, T. O. Johnson, A. Nagata, C. Almaden, S. Bailey, T. E. Ballard, L. Bernier, H. Cheng, S. Cho-Schultz, D. Dalvie, J. G. Deal, D. M. Dinh, M. P. Edwards, R. A. Ferre, K. S. Gajiwala, M. Hemkens, R. S. Kania, J. C. Kath, J. Matthews, B. W. Murray, S. Niessen, S. T. M. Orr, M. Pairish,

N. W. Sach, H. Shen, M. Shi, J. Solowiej, K. Tran, E. Tseng, P. Vicini, Y. Wang, S. L. Weinrich, R. Zhou, M. Zientek, L. Liu, Y. Luo, S. Xin, C. Zhang and J. Lafontaine, *J. Med. Chem.*, 2017, **60**, 3002–3019.

44 S. Niessen, M. M. Dix, S. Barbas, Z. E. Potter, S. Y. Lu, O. Brodsky, S. Planken, D. Behenna, C. Almaden, K. S. Gajiwala, K. Ryan, R. Ferre, M. R. Lazear, M. M. Hayward, J. C. Kath and B. F. Cravatt, *Cell Chem. Biol.*, 2017, **24**, 1388–1400.

45 J. C. Byrd, B. Harrington, S. O'Brien, J. A. Jones, A. Schuh, S. Devereux, J. Chaves, W. G. Wierda, F. T. Awan, J. R. Brown, P. Hillmen, D. M. Stephens, P. Ghia, J. C. Barrientos, J. M. Pagel, J. Woyach, D. Johnson, J. Huang, X. Wang, A. Kaptein, B. J. Lannutti, T. Covey, M. Fardis, J. McGreivy, A. Hamdy, W. Rothbaum, R. Izumi, T. G. Diacovo, A. J. Johnson and R. R. Furman, *N. Engl. J. Med.*, 2016, **374**, 323–332.

46 N. Shindo, H. Fuchida, M. Sato, K. Watari, T. Shibata, K. Kuwata, C. Miura, K. Okamoto, Y. Hatsuyama, K. Tokunaga, S. Sakamoto, S. Morimoto, Y. Abe, M. Shiroishi, J. M. M. Caaveiro, T. Ueda, T. Tamura, N. Matsunaga, T. Nakao, S. Koyanagi, S. Ohdo, Y. Yamaguchi, I. Hamachi, M. Ono and A. Ojida, *Nat. Chem. Biol.*, 2019, **15**, 250–258.

47 A. M. Manning and R. J. Davis, *Nat. Rev. Drug Discovery*, 2003, **2**, 554–565.

48 L. Qian, S. Pan, J.-S. Lee, J. Ge, L. Li and S. Q. Yao, *Chem. Commun.*, 2019, **55**, 1092–1095.

49 G. F. Desrochers, C. Cornacchia, C. S. McKay and J. P. Pezacki, *ACS Infect. Dis.*, 2018, **4**, 752–757.

50 J. E. Burke, *Mol. Cell*, 2018, **71**, 653–673.

51 S. C. Stolze, N. Liu, R. H. Wijdeven, A. W. Tuin, A. M. C. H. van den Nieuwendijk, B. I. Florea, M. van der Stelt, G. A. van der Marel, J. J. Neefjes and H. S. Overkleeft, *Mol. BioSyst.*, 2016, **12**, 1809–1817.

52 E. K. Grant, D. J. Fallon, H. C. Eberl, K. G. M. Fantom, F. Zappacosta, C. Messenger, N. C. O. Tomkinson and J. T. Bush, *Angew. Chem., Int. Ed.*, 2019, **131**, 17483–17488.

53 Q. Zhao, X. Ouyang, X. Wan, K. S. Gajiwala, J. C. Kath, L. H. Jones, A. L. Burlingame and J. Taunton, *J. Am. Chem. Soc.*, 2017, **139**, 680–685.

54 A. Cuesta, X. Wan, A. L. Burlingame and J. Taunton, *J. Am. Chem. Soc.*, 2020, **142**, 3392–3400.

55 X. Wan, T. Yang, A. Cuesta, X. Pang, T. E. Balius, J. J. Irwin, B. K. Shoichet and J. Taunton, *J. Am. Chem. Soc.*, 2020, **142**, 4960–4964.

56 M. Drag and G. S. Salvesen, *Nat. Rev. Drug Discovery*, 2010, **9**, 690–701.

57 G. Blum, S. R. Mullins, K. Keren, M. Fonovic, C. Jedeszko, M. J. Rice, B. F. Sloane and M. Bogyo, *Nat. Chem. Biol.*, 2005, **1**, 203–209.

58 M. Hu, L. Li, H. Wu, Y. Su, P. Y. Yang, M. Uttamchandani, Q. H. Xu and S. Q. Yao, *J. Am. Chem. Soc.*, 2011, **133**, 12009–12020.

59 J. C. Widen, M. Tholen, J. J. Yim, A. Antaris, K. M. Casey, S. Rogalla, A. Klaassen, J. Sorger and M. Bogyo, *Nat. Biomed. Eng.*, 2021, **5**, 264–277.

60 J. B. Denault and G. S. Salvesen, *Methods Mol. Biol.*, 2008, **414**, 191–220.

61 N. Aggarwal and B. F. Sloane, *Proteonomics Clin. Appl.*, 2014, **8**, 427–437.

62 L. E. Edgington, A. B. Berger, G. Blum, V. E. Albrow, M. G. Paulick, N. Lineberry and M. Bogyo, *Nat. Med.*, 2009, **15**, 967–973.

63 L. E. Edgington, M. Verdoes, A. Ortega, N. P. Withana, J. Lee, S. Syed, M. H. Bachmann, G. Blum and M. Bogyo, *J. Am. Chem. Soc.*, 2013, **135**, 174–182.

64 Y. Shaulov-Rotem, E. Merquiol, T. Weiss-Sadan, O. Moshel, S. Salpeter, D. Shabat, F. Kaschani, M. Kaiser and G. Blum, *Chem. Sci.*, 2016, **7**, 1322–1337.

65 K. B. Sexton, M. D. Witte, G. Blum and M. Bogyo, *Bioorg. Med. Chem. Lett.*, 2007, **17**, 649–653.

66 M. Poreba, K. Groborz, M. Vizovisek, M. Maruggi, D. Turk, B. Turk, G. Powis, M. Drag and G. S. Salvesen, *Chem. Sci.*, 2019, **10**, 8461–8477.

67 N. Amara, I. T. Foe, O. Onguka, M. Garland and M. Bogyo, *Cell Chem. Biol.*, 2019, **26**, 35–47.

68 M. Tholen, J. J. Yim, K. Groborz, E. Yoo, B. A. Martin, N. S. van den Berg, M. Drag and M. Bogyo, *Angew. Chem., Int. Ed.*, 2020, **59**, 19143–19152.

69 E. Walker, Y. Liu, I. Kim, M. Biro, S. R. Iyer, H. Ezaldein, J. Scott, M. Merati, R. Mistur, B. Zhou, B. Straight, J. J. Yim, M. Bogyo, M. Mann, D. L. Wilson, J. P. Basilion and D. L. Popkin, *Cancer Res.*, 2020, **80**, 2045–2055.

70 L. O. Ofori, N. P. Withana, T. R. Prestwood, M. Verdoes, J. J. Brady, M. M. Winslow, J. Sorger and M. Bogyo, *ACS Chem. Biol.*, 2015, **10**, 1977–1988.

71 F. V. Suurs, S. Q. Qiu, J. J. Yim, C. P. Schroder, H. Timmer-Bosscha, E. S. Bensen, J. T. Santini Jr, E. G. E. de Vries, M. Bogyo and G. M. van Dam, *EJNMMI Res.*, 2020, **10**, 111.

72 M. Verdoes, K. Oresic Bender, E. Segal, W. A. van der Linden, S. Syed, N. P. Withana, L. E. Sanman and M. Bogyo, *J. Am. Chem. Soc.*, 2013, **135**, 14726–14730.

73 A. Page-McCaw, A. J. Ewald and Z. Werb, *Nat. Rev. Mol. Cell Biol.*, 2007, **8**, 221–233.

74 M. Morell, T. Nguyen Duc, A. L. Willis, S. Syed, J. Lee, E. Deu, Y. Deng, J. Xiao, B. E. Turk, J. R. Jessen, S. J. Weiss and M. Bogyo, *J. Am. Chem. Soc.*, 2013, **135**, 9139–9148.

75 N. Amara, M. Tholen and M. Bogyo, *ACS Chem. Biol.*, 2018, **13**, 2645–2654.

76 L. Wu, Z. Armstrong, S. P. Schroder, C. de Boer, M. Artola, J. M. Aerts, H. S. Overkleeft and G. J. Davies, *Curr. Opin. Chem. Biol.*, 2019, **53**, 25–36.

77 V. Cullen, S. P. Sardi, J. Ng, Y. H. Xu, Y. Sun, J. J. Tomlinson, P. Kolodziej, I. Kahn, P. Saftig, J. Woulfe, J. C. Rochet, M. A. Glicksman, S. H. Cheng, G. A. Grabowski, L. S. Shihabuddin and M. G. Schlossmacher, *Ann. Neurol.*, 2011, **69**, 940–953.

78 M. Czjzek, M. Cicek, V. Zamboni, D. R. Bevan, B. Henrissat and A. Esen, *Proc. Natl. Acad. Sci. U. S. A.*, 2000, **97**, 13555–13560.

79 B. Bissaro, P. Monsan, R. Faure and M. J. O'Donohue, *Biochem. J.*, 2015, **467**, 17–35.

80 W. W. Kallemeijn, K.-Y. Li, M. D. Witte, A. R. A. Marques, J. Aten, S. Scheij, J. Jiang, L. I. Willems, T. M. Voorn-Brouwer, C. P. A. A. van Roomen, R. Ottenhoff, R. G. Boot, H. van den Elst, M. T. C. Walvoort, B. I. Florea, J. D. C. Codee, G. A. van der Marel, J. M. F. G. Aerts and H. S. Overkleeft, *Angew. Chem., Int. Ed.*, 2012, **51**, 12529–12533.

81 L. I. Willems, T. J. M. Beenakker, B. Murray, S. Scheij, W. W. Kallemeijn, R. G. Boot, M. Verhoek, W. E. Donker-Koopman, M. J. Ferraz, E. R. van Rijssel, B. I. Florea, J. D. C. Codee, G. A. van der Marel, J. M. F. G. Aerts and H. S. Overkleeft, *J. Am. Chem. Soc.*, 2014, **136**, 11622–11625.

82 B. T. Adams, S. Niccoli, M. A. Chowdhury, A. N. K. Esarik, S. J. Lees, B. P. Rempel and C. P. Phenix, *Chem. Commun.*, 2015, **51**, 11390–11393.

83 A. Alcaide, A. Trapero, Y. Perez and A. Llebaria, *Org. Biomol. Chem.*, 2015, **13**, 5690–5697.

84 J. Jiang, T. J. M. Beenakker, W. W. Kallemeijn, G. A. van der Marel, H. van den Elst, J. D. C. Codee, J. M. F. G. Aerts and H. S. Overkleeft, *Chem. - Eur. J.*, 2015, **21**, 10861–10869.

85 T. M. Gloster, R. Madsen and G. J. Davies, *Org. Biomol. Chem.*, 2007, **5**, 444–446.

86 M. D. Witte, W. W. Kallemeijn, J. Aten, K. Y. Li, A. Strijland, W. E. Donker-Koopman, A. M. van den Nieuwendijk, B. Bleijlevens, G. Kramer, B. I. Florea, B. Hooibrink, C. E. Hollak, R. Ottenhoff, R. G. Boot, G. A. van der Marel, H. S. Overkleeft and J. M. Aerts, *Nat. Chem. Biol.*, 2010, **6**, 907–913.

87 D. J. Vocadlo, H. C. Hang, E. J. Kim, J. A. Hanover and C. R. Bertozzi, *Proc. Natl. Acad. Sci. U. S. A.*, 2003, **100**, 9116–9121.

88 S. J. Williams, V. Notenboom, J. Wicki, D. R. Rose and S. G. Withers, *J. Am. Chem. Soc.*, 2000, **122**, 4229–4230.

89 R. O. Brady, J. N. Kanfer, R. M. Bradley and D. Shapiro, *J. Clin. Invest.*, 1966, **45**, 1112–1115.

90 E. van Meel, E. Bos, M. J. C. van der Lienden, H. S. Overkleeft, S. I. van Kasteren, A. J. Koster and J. M. F. G. Aerts, *Traffic*, 2019, **20**, 346–356.

91 J. E. Deane, S. C. Graham, N. N. Kim, P. E. Stein, R. McNair, M. B. Cachon-Gonzalez, T. M. Cox and R. J. Read, *Proc. Natl. Acad. Sci. U. S. A.*, 2011, **108**, 15169–15173.

92 A. R. Marques, L. I. Willems, M. D. Herrera, B. I. Florea, S. Scheij, R. Ottenhoff, C. P. van Roomen, M. Verhoek, J. K. Nelson, W. W. Kallemeijn, A. Biela-Banas, O. R. Martin, M. B. Cachon-Gonzalez, N. N. Kim, T. M. Cox, R. G. Boot, H. S. Overkleeft and J. M. Aerts, *Chembiochem*, 2017, **18**, 402–412.

93 M. Artola, C.-L. Kuo, L. T. Lelieveld, R. J. Rowland, G. A. van der Marel, J. D. C. Codée, R. G. Boot, G. J. Davies, J. M. F. G. Aerts and H. S. Overkleeft, *J. Am. Chem. Soc.*, 2019, **141**, 4214–4218.

94 L. Wu, J. Jiang, Y. Jin, W. W. Kallemeijn, C.-L. Kuo, M. Artola, W. Dai, C. van Elk, M. van Eijk, G. A. van der Marel, J. D. C. Codée, B. I. Florea, J. M. F. G. Aerts, H. S. Overkleeft and G. J. Davies, *Nat. Chem. Biol.*, 2017, **13**, 867–873.

95 H. Van den Hout, A. J. Reuser, A. G. Vulto, M. C. Loonen, A. Cromme-Dijkhuis and A. T. Van der Ploeg, *Lancet*, 2000, **356**, 397–398.

96 J. Jiang, C. L. Kuo, L. Wu, C. Franke, W. W. Kallemeijn, B. I. Florea, E. van Meel, G. A. van der Marel, J. D. Codee, R. G. Boot, G. J. Davies, H. S. Overkleeft and J. M. Aerts, *ACS Cent. Sci.*, 2016, **2**, 351–358.

97 Y. Chen, Z. Armstrong, M. Artola, B. I. Florea, C. L. Kuo, C. de Boer, M. S. Rasmussen, M. Abou Hachem, G. A. van der Marel, J. D. C. Codee, J. Aerts, G. J. Davies and H. S. Overkleeft, *J. Am. Chem. Soc.*, 2021, **143**, 2423–2432.

98 S. P. Schroder, C. de Boer, N. G. S. McGregor, R. J. Rowland, O. Moroz, E. Blagova, J. Reijngoud, M. Arentshorst, D. Osborn, M. D. Morant, E. Abbate, M. A. Stringer, K. Krogh, L. Raich, C. Rovira, J. G. Berrin, G. P. van Wezel, A. F. J. Ram, B. I. Florea, G. A. van der Marel, J. D. C. Codee, K. S. Wilson, L. Wu, G. J. Davies and H. S. Overkleeft, *ACS Cent. Sci.*, 2019, **5**, 1067–1078.

99 C. Whidbey, N. C. Sadler, R. N. Nair, R. F. Volk, A. J. DeLeon, L. M. Bramer, S. J. Fansler, J. R. Hansen, A. K. Shukla, J. K. Jansson, B. D. Thrall and A. T. Wright, *J. Am. Chem. Soc.*, 2018, **141**, 42–47.

100 A. Hershko and A. Ciechanover, *Annu. Rev. Biochem.*, 1998, **67**, 425–479.

101 M. Bogyo, J. S. McMaster, M. Gaczynska, D. Tortorella, A. L. Goldberg and H. Ploegh, *Proc. Natl. Acad. Sci. U. S. A.*, 1997, **94**, 6629–6634.

102 B. H. B. K. Lihao Meng, N. Sin and C. M. Crews, *Cancer Res.*, 1999, **59**, 2798–2801.

103 H. Ovaa, P. F. van Swieten, B. M. Kessler, M. A. Leeuwenburgh, E. Fiebiger, A. M. van den Nieuwendijk, P. J. Galardy, G. A. van der Marel, H. L. Ploegh and H. S. Overkleeft, *Angew. Chem., Int. Ed.*, 2003, **42**, 3626–3629.

104 G. de Bruin, B. T. Xin, M. Kraus, M. van der Stelt, G. A. van der Marel, A. F. Kisselev, C. Driessen, B. I. Florea and H. S. Overkleeft, *Angew. Chem., Int. Ed.*, 2016, **55**, 4199–4203.

105 J. A. Ward, L. McLellan, M. Stockley, K. R. Gibson, G. A. Whitlock, C. Knights, J. A. Harrigan, X. Jacq and E. W. Tate, *ACS Chem. Biol.*, 2016, **11**, 3268–3272.

106 N. Panyain, A. Godinat, T. Lanyon-Hogg, S. Lachiondo-Ortega, E. J. Will, C. Soudy, M. Mondal, K. Mason, S. Elkhalifa, L. M. Smith, J. A. Harrigan and E. W. Tate, *J. Am. Chem. Soc.*, 2020, **142**, 12020–12026.

107 B. A. Gibson and W. L. Kraus, *Nat. Rev. Mol. Cell Biol.*, 2012, **13**, 411–424.

108 R. T. Howard, P. Hemsley, P. Petteruti, C. N. Saunders, J. A. Molina Bermejo, J. S. Scott, J. W. Johannes and E. W. Tate, *ACS Chem. Biol.*, 2020, **15**, 325–333.

109 C. S. Lentz, J. R. Sheldon, L. A. Crawford, R. Cooper, M. Garland, M. R. Amieva, E. Weerapana, E. P. Skaar and M. Bogyo, *Nat. Chem. Biol.*, 2018, **14**, 609–617.

110 A. C. M. van Esbroeck, A. P. A. Janssen, A. B. R. Cognetta, D. Ogasawara, G. Shpak, M. van der Kroeg, V. Kantae, M. P. Baggelaar, F. M. S. de Vrij, H. Deng, M. Allara, F. Fezza, Z. Lin, T. van der Wel, M. Soethoudt,

E. D. Mock, H. den Dulk, I. L. Baak, B. I. Florea, G. Hendriks, L. De Petrocellis, H. S. Overkleeft, T. Hankemeier, C. I. De Zeeuw, V. Di Marzo, M. Maccarrone, B. F. Cravatt, S. A. Kushner and M. van der Stelt, *Science*, 2017, **356**, 1084–1087.

111 Z. Huang, D. Ogasawara, U. I. Seneviratne, A. B. Cognetta, C. W. Am Ende, D. M. Nason, K. Lapham, J. Litchfield, D. S. Johnson and B. F. Cravatt, *ACS Chem. Biol.*, 2019, **14**, 192–197.

112 R. E. Rau, B. A. Rodriguez, M. Luo, M. Jeong, A. Rosen, J. H. Rogers, C. T. Campbell, S. R. Daigle, L. S. Deng, Y. C. Song, S. Sweet, T. Chevassut, M. Andreeff, S. M. Kornblau, W. Li and M. A. Goodell, *Blood*, 2016, **128**, 971–981.

113 B. Zhu, H. Zhang, S. Pan, C. Wang, J. Ge, J.-S. Lee and S. Q. Yao, *Chem.–Asian J.*, 2016, **22**, 7824–7836.

114 M. E. Pacold, K. R. Brimacombe, S. H. Chan, J. M. Rohde, C. A. Lewis, L. J. Swier, R. Possemato, W. W. Chen, L. B. Sullivan, B. P. Fiske, S. Cho, E. Freinkman, K. Birsoy, M. Abu-Remaileh, Y. D. Shaul, C. M. Liu, M. Zhou, M. J. Koh, H. Chung, S. M. Davidson, A. Luengo, A. Q. Wang, X. Xu, A. Yasgar, L. Liu, G. Rai, K. D. Westover, M. G. Vander Heiden, M. Shen, N. S. Gray, M. B. Boxer and D. M. Sabatini, *Nat. Chem. Biol.*, 2016, **12**, 452–458.

115 S. Pan, S.-Y. Jang, S. S. Liew, J. Fu, D. Wang, J.-S. Lee and S. Q. Yao, *Angew. Chem., Int. Ed.*, 2018, **57**, 579–583.

116 L. L. Lairson, B. Henrissat, G. J. Davies and S. G. Withers, *Annu. Rev. Biochem.*, 2008, **77**, 521–555.

117 A. Richman, A. Swanson, T. Humphrey, R. Chapman, B. McGarvey, R. Pocs and J. Brandle, *Plant J.*, 2005, **41**, 56–67.

118 Y. Zhou, W. Li, W. You, Z. Di, M. Wang, H. Zhou, S. Yuan, N.-K. Wong and Y. Xiao, *Chem. Commun.*, 2018, **54**, 7179–7182.

119 N.-K. Wong, S. Zhong, W. Li, F. Zhou, Z. Deng and Y. Zhou, *Chem. Commun.*, 2020, **56**, 12387–12390.

120 L. Mouchiroud, R. H. Houtkooper, N. Moullan, E. Katsyuba, D. Ryu, C. Canto, A. Mottis, Y. S. Jo, M. Viswanathan, K. Schoonjans, L. Guarente and J. Auwerx, *Cell*, 2013, **154**, 430–441.

121 A. Ray Chaudhuri and A. Nussenzweig, *Nat. Rev. Mol. Cell Biol.*, 2017, **18**, 610–621.

122 H. Jiang, J. H. Kim, K. M. Frizzell, W. L. Kraus and H. Lin, *J. Am. Chem. Soc.*, 2010, **132**, 9363–9372.

123 A. Buntz, S. Wallrodt, E. Gwosch, M. Schmalz, S. Beneke, E. Ferrando-May, A. Marx and A. Zumbusch, *Angew. Chem., Int. Ed.*, 2016, **55**, 11256–11260.

124 M. C. Morris, J. Depollier, J. Mery, F. Heitz and G. Divita, *Nat. Biotechnol.*, 2001, **19**, 1173–1176.

125 S. Wallrodt, A. Buntz, Y. Wang, A. Zumbusch and A. Marx, *Angew. Chem., Int. Ed.*, 2016, **55**, 7660–7664.

126 S. Wallrodt, E. L. Simpson and A. Marx, *Beilstein J. Org. Chem.*, 2017, **13**, 495–501.

127 C. Canto, R. H. Houtkooper, E. Pirinen, D. Y. Youn, M. H. Oosterveer, Y. Cen, P. J. Fernandez-Marcos, H. Yamamoto, P. A. Andreux, P. Cettour-Rose, K. Gademann, C. Rinsch, K. Schoonjans, A. A. Sauve and J. Auwerx, *Cell Metab.*, 2012, **15**, 838–847.

128 M. Grammel, H. Hang and N. K. Conrad, *Chembiochem*, 2012, **13**, 1112–1115.

129 N. P. Westcott, J. P. Fernandez, H. Molina and H. C. Hang, *Nat. Chem. Biol.*, 2017, **13**, 302–308.

130 K. Kalesh, S. Lukauskas, A. J. Borg, A. P. Snijders, V. Ayyappan, A. K. L. Leung, D. O. Haskard and P. A. DiMaggio, *Sci. Rep.*, 2019, **9**, 6655.

131 X.-N. Zhang, Q. Cheng, J. Chen, A. T. Lam, Y. Lu, Z. Dai, H. Pei, N. M. Evdokimov, S. G. Louie and Y. Zhang, *Nat. Commun.*, 2019, **10**, 4196.

132 D. Koley and A. J. Bard, *Proc. Natl. Acad. Sci. U. S. A.*, 2010, **107**, 16783–16787.

133 I. Carter-O'Connell, H. Jin, R. K. Morgan, L. L. David and M. S. Cohen, *J. Am. Chem. Soc.*, 2014, **136**, 5201–5204.

134 B. A. Gibson, Y. J. Zhang, H. Jiang, K. M. Hussey, J. H. Shrimp, H. N. Lin, F. Schwede, Y. H. Yu and W. L. Kraus, *Science*, 2016, **353**, 45–50.

135 A. T. Lam, X. N. Zhang, V. V. Courouble, T. S. Strutzenberg, H. Pei, B. L. Stiles, S. G. Louie, P. R. Griffin and Y. Zhang, *ACS Chem. Biol.*, 2021, **16**, 389–396.

136 J. Sileikyte, S. Sundalam, L. L. David and M. S. Cohen, *J. Am. Chem. Soc.*, 2021, **143**, 6787–6791.

137 F. Ikeda, N. Crosetto and I. Dikic, *Cell*, 2010, **143**, 677–681.

138 J. A. Harrigan, X. Jacq, N. M. Martin and S. P. Jackson, *Nat. Rev. Drug Discovery*, 2018, **17**, 57–78.

139 D. Flierman, G. J. van der Heden Van Noort, R. Ekkebus, P. P. Geurink, T. E. T. Mevissen, M. K. Hospenthal, D. Komander and H. Ovaa, *Cell Chem. Biol.*, 2016, **23**, 472–482.

140 S. D. Whedon, N. Markandeya, A. S. J. B. Rana, N. A. Senger, C. E. Weller, F. Tureček, E. R. Strieter and C. Chatterjee, *J. Am. Chem. Soc.*, 2016, **138**, 13774–13777.

141 J. Liang, L. Zhang, X.-L. Tan, Y.-K. Qi, S. Feng, H. Deng, Y. Yan, J.-S. Zheng, L. Liu and C.-L. Tian, *Angew. Chem., Int. Ed.*, 2017, **56**, 2744–2748.

142 P. Xu, D. M. Duong, N. T. Seyfried, D. Cheng, Y. Xie, J. Robert, J. Rush, M. Hochstrasser, D. Finley and J. Peng, *Cell*, 2009, **137**, 133–145.

143 R. Meledin, S. M. Mali, O. Kleifeld and A. Brik, *Angew. Chem., Int. Ed.*, 2018, **57**, 5645–5649.

144 J. R. Shaeffer, *J. Biol. Chem.*, 1994, **269**, 22205–22210.

145 J. Liu, C. F. Han, B. Xie, Y. Wu, S. X. Liu, K. Chen, M. Xia, Y. Zhang, L. J. Song, Z. Q. Li, T. Zhang, F. Ma, Q. Q. Wang, J. L. Wang, K. J. Deng, Y. Zhuang, X. H. Wu, Y. Z. Yu, T. Xu and X. T. Cao, *Nat. Immunol.*, 2014, **15**, 612–622.

146 T. P. Yang, X. M. Li, X. C. Bao, Y. M. E. Fung and X. D. Li, *Nat. Chem. Biol.*, 2016, **12**, 70–72.

147 X.-D. Tan, M. Pan, S. Gao, Y. Zheng, J. Shi and Y.-M. Li, *Chem. Commun.*, 2017, **53**, 10208–10211.

148 W. Gui, C. A. Ott, K. Yang, J. S. Chung, S. Shen and Z. Zhuang, *J. Am. Chem. Soc.*, 2018, **140**, 12424–12433.

149 G. Saito, J. A. Swanson and K. D. Lee, *Adv. Drug Delivery Rev.*, 2003, **55**, 199–215.

150 Z. Q. Li, L. H. Qian, L. Li, J. C. Bernhammer, H. V. Huynh, J. S. Lee and S. Q. Yao, *Angew. Chem., Int. Ed.*, 2016, **55**, 2002–2006.
151 W. Gui, S. Shen and Z. Zhuang, *J. Am. Chem. Soc.*, 2020, **142**, 19493–19501.
152 Y. J. Machida, Y. Machida, A. A. Vashisht, J. A. Wohlschlegel and A. Dutta, *J. Biol. Chem.*, 2009, **284**, 34179–34188.
153 X. L. Zhuo, X. Guo, X. Y. Zhang, G. H. Jing, Y. Wang, Q. Chen, Q. Jiang, J. J. Liu and C. M. Zhang, *J. Cell Biol.*, 2015, **210**, 727–735.
154 M. P. C. Mulder, K. Witting, I. Berlin, J. N. Pruneda, K.-P. Wu, J.-G. Chang, R. Merkx, J. Bialas, M. Groettrup, A. C. O. Vertegaal, B. A. Schulman, D. Komander, J. Neefjes, F. El Oualid and H. Ovaa, *Nat. Chem. Biol.*, 2016, **12**, 523–530.
155 C. M. Pickart, E. M. Kasperek, R. Beal and A. Kim, *J. Biol. Chem.*, 1994, **269**, 7115–7123.
156 K.-C. Pao, N. T. Wood, A. Knebel, K. Rafie, M. Stanley, P. D. Mabbitt, R. Sundaramoorthy, K. Hofmann, D. M. F. van Aalten and S. Virdee, *Nature*, 2018, **556**, 381–385.
157 S. Minucci and P. G. Pelicci, *Nat. Rev. Cancer*, 2006, **6**, 38–51.
158 Y. Xie, J. Ge, H. Lei, B. Peng, H. Zhang, D. Wang, S. Pan, G. Chen, L. Chen, Y. Wang, Q. Hao, S. Q. Yao and H. Sun, *J. Am. Chem. Soc.*, 2016, **138**, 15596–15604.
159 P. Bheda, H. Jing, C. Wolberger and H. N. Lin, *Annu. Rev. Biochem.*, 2016, **85**, 405–429.
160 M. D. Spalding and S. T. Prigge, *Microbiol. Mol. Biol. Rev.*, 2010, **74**, 200–228.
161 Y. Xie, L. Chen, R. Wang, J. Wang, J. Li, W. Xu, Y. Li, S. Q. Yao, L. Zhang, Q. Hao and H. Sun, *J. Am. Chem. Soc.*, 2019, **141**, 18428–18436.
162 Y. Fu, D. Dominissini, G. Rechavi and C. He, *Nat. Rev. Genet.*, 2014, **15**, 293–306.
163 Y. N. Xing, Z. Li, Y. Chen, J. B. Stock, P. D. Jeffrey and Y. G. Shi, *Cell*, 2008, **133**, 154–163.
164 T. C. Petrossian and S. G. Clarke, *Mol. Cell. Proteomics*, 2011, **10**, M110.000976.
165 S. C. Lu, *Int. J. Biochem. Cell Biol.*, 2000, **32**, 391–395.
166 C. Dalhoff, M. Huben, T. Lenz, P. Poot, E. Nordhoff, H. Koster and E. Weinhold, *Chembiochem*, 2010, **11**, 256–265.
167 B. D. Horning, R. M. Suciu, D. A. Ghadiri, O. A. Ulanovskaya, M. L. Matthews, K. M. Lum, K. M. Backus, S. J. Brown, H. Rosen and B. F. Cravatt, *J. Am. Chem. Soc.*, 2016, **138**, 13335–13343.
168 J. S. Takahashi, L. H. Pinto and M. H. Vitaterna, *Science*, 1994, **264**, 1724–1733.
169 C. G. Parker, A. Galmozzi, Y. Wang, B. E. Correia, K. Sasaki, C. M. Joslyn, A. S. Kim, C. L. Cavallaro, R. M. Lawrence, S. R. Johnson, I. Narvaiza, E. Saez and B. F. Cravatt, *Cell*, 2017, **168**, 527–541.
170 S. M. Hacker, K. M. Backus, M. R. Lazear, S. Forli, B. E. Correia and B. F. Cravatt, *Nat. Chem.*, 2017, **9**, 1181–1190.
171 M. Shrivastav, E. Gounaris, M. W. Khan, J. Ko, S. H. Ryu, M. Bogyo, A. Larson, T. A. Barret and D. J. Bentrem, *PloS One*, 2018, **13**, e0206568.
172 Z. Shi, X. Han, W. Hu, H. Bai, B. Peng, L. Ji, Q. Fan, L. Li and W. Huang, *Chem. Soc. Rev.*, 2020, **49**, 7533–7567.
173 F. Zhang and Z. Lei, *Angew. Chem., Int. Ed.*, 2020, DOI: 10.1002/anie.202007040.
174 M. N. Gandy, A. W. Debowski and K. A. Stubbs, *Chem. Commun.*, 2011, **47**, 5037–5039.
175 S. E. Dettling, M. Ahmadi, Z. Lin, L. He and M. L. Matthews, *Curr. Protoc. Chem. Biol.*, 2020, **12**, e86.